Proton Spin Structure in Run Group C

Derek Holmberg
7-9-25

CLAS Collaboration Meeting July 8-11

Where Does the Proton Spin Come From?

- Total proton spin $\frac{1}{2} = quark\ spin + gluon\ spin + quark\ orbital\ momentum + gluon\ orbital\ momentum$
- Quark spin contribution depends on polarized parton distribution functions (PDFs)
- **Polarized PDF**: $\Delta q_i(x) = q_i^{\uparrow}(x) - q_i^{\downarrow}(x)$
- $g_1(x) = \frac{1}{2}\Sigma_i e_i^2 \Delta q_i(x) \propto \frac{1}{2}\left[\frac{4}{9}\Delta u(x) + \frac{1}{9}\Delta d(x) + \frac{1}{9}\Delta s(x) + \cdots\right]$
- Probed through polarized electron-proton scattering

Proton total spin $|\hat{S}| = \hbar/2$

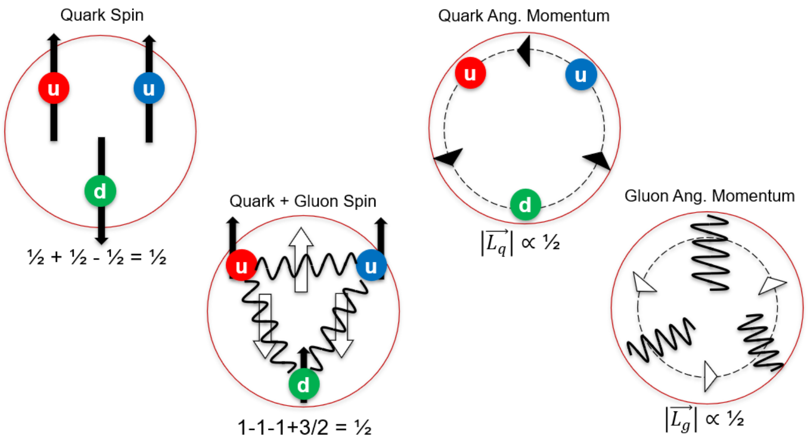

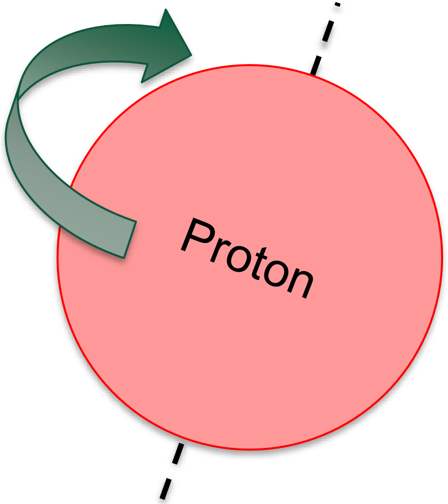

Polarized *ep* Scattering

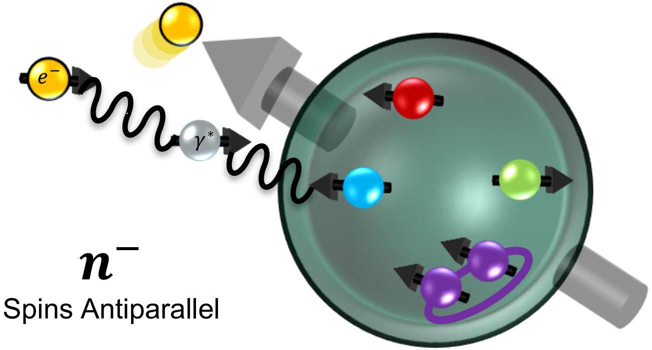

$\boldsymbol{n^-}$

Spins Antiparallel

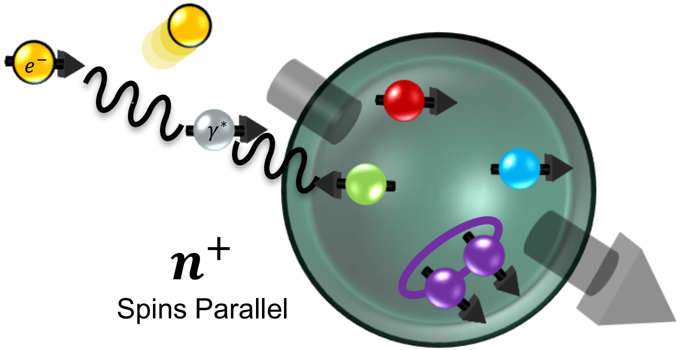

$\boldsymbol{n^+}$

Spins Parallel

- Protons are polarized either parallel or antiparallel to the beam electrons' spins
- Deep inelastic scattering (DIS): electrons scatter off individual quarks ($Q^2 > 1\ \mathrm{GeV}^2, \quad W > 2\ \mathrm{GeV}$)
- Scattering conserves spin (angular momentum), so any asymmetry between $n^{\pm}$ is related to spin structure

$$A_{||}(x, Q^2) = \frac{n^- - n^+}{n^- + n^+} = D\big(A_1(x, Q^2) + \eta A_2(x, Q^2)\big)$$

- With $A_1, A_2 =$ virtual photon asymmetries

$$A_1(x, Q^2) \propto \frac{g_1(x, Q^2)}{F_1(x, Q^2)} = \frac{\Sigma_i e_i^2 \Delta q_i(x, Q^2)}{\Sigma_i e_i^2 q_i(x, Q^2)}$$

The CLAS12 Detector

- Inclusive electron scattering: $ep \to eX$, $ed \to eX$
- Consider electrons in the Forward Detector (FD): Drift chambers, ECAL, HTCC
- Electron EB PID:
  - Negative track in the DC (inbending data)
  - $E_{PCAL} > 60\ MeV$
  - Photoelectrons in HTCC $nphe > 2$
- Deep inelastic kinematic cuts:
  - $Q^2 > 1\ \text{GeV}^2, W > 2\ \text{GeV},$
  - $E' > 2.6\ \text{GeV}$ (minimize radiative effects)
- Fiducial cuts (work in progress):
  - $-10\ cm < V_Z < 2\ cm,\ 5° < \theta < 40°,\ |\chi^2_{PID}| < 3$
  - Investigating DC edge variable cut (edge>5 cm)
  - Investigating ECAL lu, lv, lw strip cuts

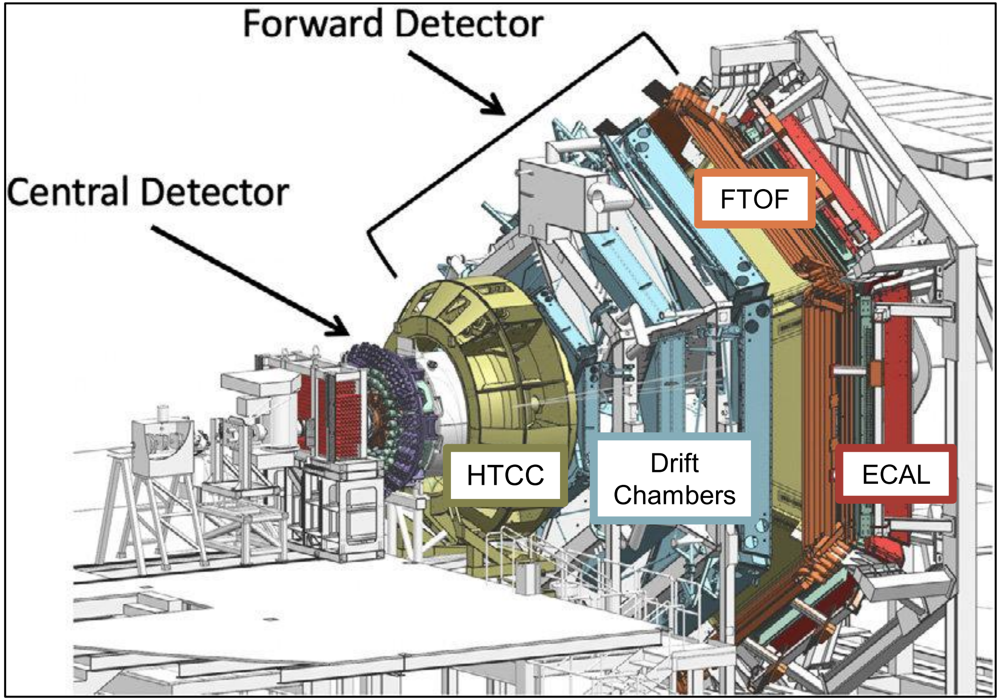

Diagram of CLAS12 Detector, Ziegler et. al.

The CLAS12 Detector

- Inclusive electron scattering: $ep \to eX,\ ed \to eX$
- Consider electrons in the Forward Detector (FD): Drift chambers, ECAL, HTCC
- Electron EB PID:
  - Negative track in the DC (inbending data)
  - $E_{PCAL} > 60\ MeV$
  - Photoelectrons in HTCC $nphe > 2$
- Deep inelastic kinematic cuts:
  - $Q^2 > 1\ \mathrm{GeV}^2, W > 2\ \mathrm{GeV},$
  - $E' > 2.6\ \mathrm{GeV}$ (minimize radiative effects)
- Fiducial cuts (work in progress):
  - $-10\ cm < V_Z < 2\ cm,\ 5° < \theta < 40°,\ |\chi^2_{PID}| < 3$
  - Investigating DC edge variable cut (edge>5 cm)
  - Investigating ECAL lu, lv, lw strip cuts
- Run Group C polarized target

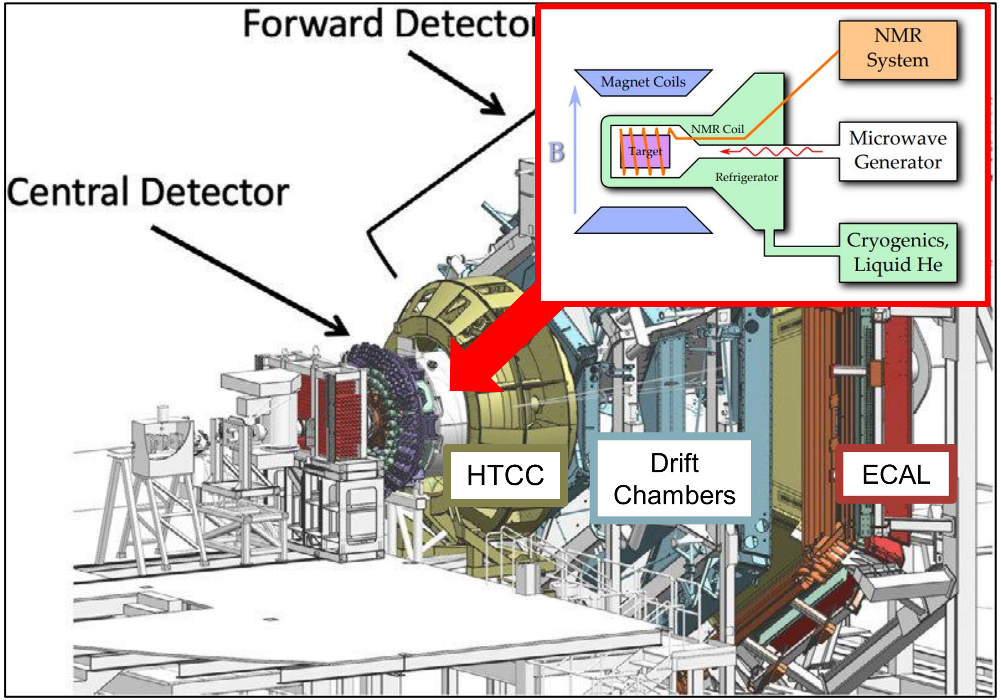

Diagram of CLAS12 Detector, Ziegler et. al.

Run Group C Polarized Target

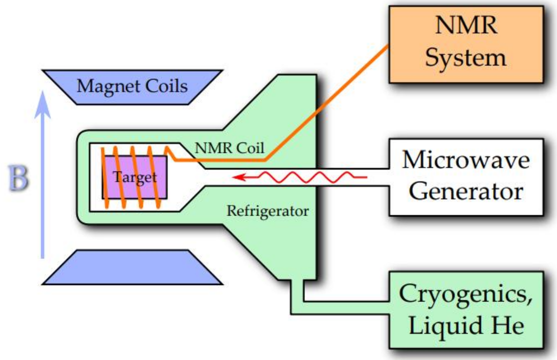

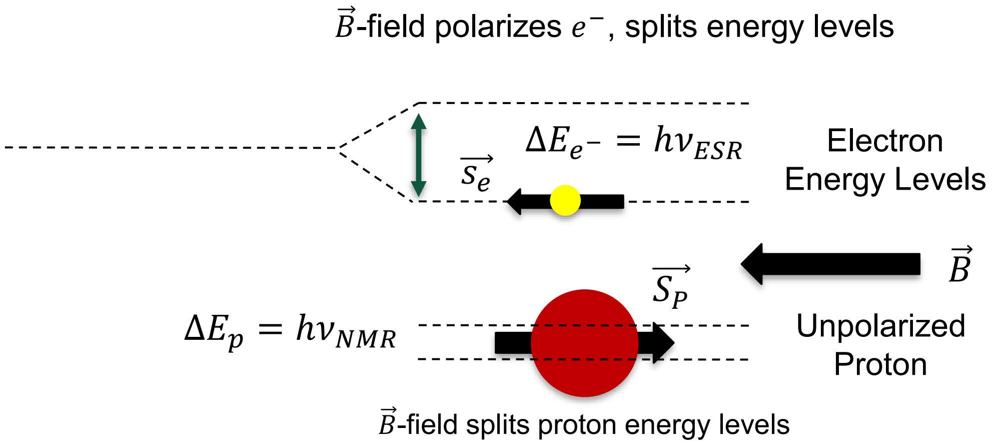

Ammonia crystals unexposed to beam (left), crystals after beam exposure (right). Purple color from paramagnetic centers.

- Target material: frozen ammonia crystals
- Ammonia chosen for use in dynamic nuclear polarization
- Expose crystals to beam, creating free electron paramagnetic centers in target
- Cool to ~1 K in a 5 T field generated by solenoid, where free electrons almost completely polarize, but protons don’t
- Exposing target to microwaves with a frequency of $\nu_{ESR} \pm \nu_{NMR}$ (~140 GHz), polarization of the electrons is transferred to the protons (or deuterons)
- ~90% for protons, ~40% for deuterons

Unpolarized Background

- In addition to polarized scattering in the target, there's a large source of unpolarized background: N, Al, He nuclei in target/bath
- Reduces measured $A_{||}$, and cannot be removed with vertex/kinematic cuts
- Quantified using a dilution factor D_F

$$D_F = \frac{Y_H}{Y_{Ammonia}} = \frac{3\sigma_H \ell_H \rho_H}{3\sigma_H \ell_H \rho_H + \sigma_N \ell_N \rho_N + \sigma_{He} \ell_{He} \rho_{He} + \sigma_{Al} \ell_{Al} \rho_{Al}}$$

- Imperfect polarization of beam electrons and target particles: $P_b P_t$

- Dividing $A_{||}$ by D_F and $P_b P_t$ accounts for the background

$$A_{||,phys} = \frac{A_{||,raw}}{D_F P_b P_t} \propto A_1$$

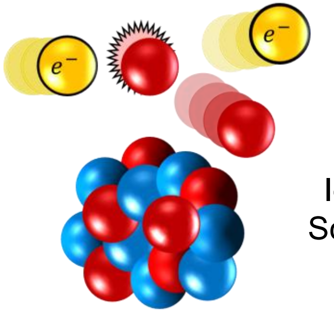

Ideal ep Scattering

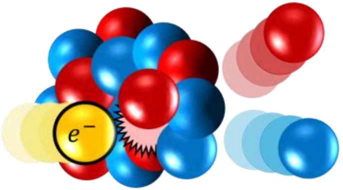

N, Al Nuclei Scattering

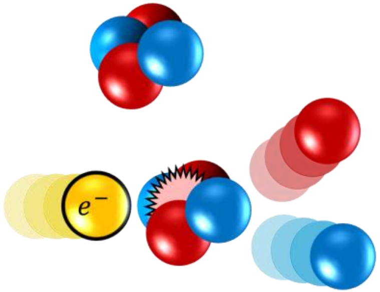

Liquid He Scattering

Unpolarized Background

- In addition to polarized scattering in the target, there's a large source of unpolarized background: N, Al, He nuclei in target/bath
- Reduces measured $A_{||}$, and cannot be removed with vertex/kinematic cuts
- Quantified using a dilution factor D_F

$$D_F = \frac{Y_H}{Y_{Ammonia}} = \frac{3\sigma_H \ell_H \rho_H}{3\sigma_H \ell_H \rho_H + \sigma_N \ell_N \rho_N + \sigma_{He} \ell_{He} \rho_{He} + \sigma_{Al} \ell_{Al} \rho_{Al}}$$

- Imperfect polarization of beam electrons and target particles: $P_b P_t$

- Dividing $A_{||}$ by D_F and $P_b P_t$ accounts for the background

$$A_{||,phys} = \frac{A_{||,raw}}{D_F P_b P_t} \propto A_1$$

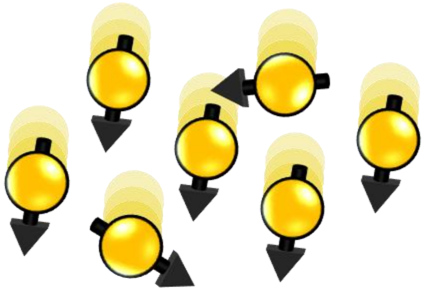

Beam Electron Polarization P_b

Target Polarization P_t

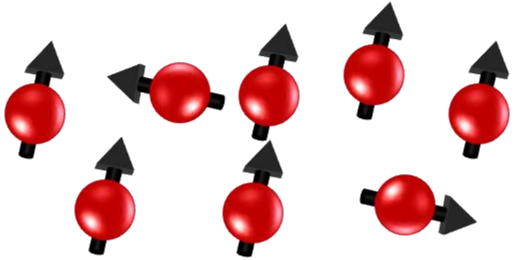

Calculating the Dilution Factor

- Advantageous to write D_F in terms of scattering counts from background targets instead of cross sections

- $n_A \propto \sigma_{Al} + \sigma_{He} + \frac{7}{6}\sigma_C + \sigma_H,$ where $\frac{7}{6}\sigma_C \approx \sigma_N$
- $n_{MT} \propto \sigma_{Al} + \sigma_{He}$
- $n_C \propto \sigma_{Al} + \sigma_{He} + \sigma_C$
- $n_{CH} \propto \sigma_{Al} + \sigma_{He} + \sigma_C + \sigma_H$
- $n_F \propto \sigma_{Al}$

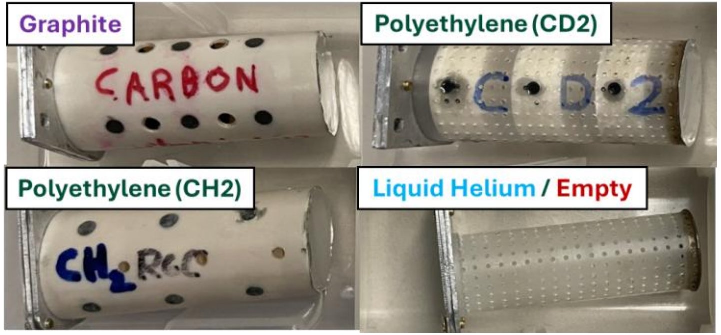

- Solving for cross sections and rewriting the D_F yields

$$D_F(x, Q^2) = P_F \frac{C_1 n_C + C_2 n_{MT} + C_3 n_{CH} + C_4 n_F}{C_5 n_A}$$

- Packing fraction P_F is the target volume fraction occupied by the ammonia crystals

$$P_F(x, Q^2) = \frac{D_1(n_A - n_{MT})}{D_2 n_{MT} + D_3 n_C + D_4 n_{CH} + D_5 n_F}$$

$C_i, D_i \propto \ell_i, \rho_i$ of target materials

Calculating the Dilution Factor

- Advantageous to write D_F in terms of scattering counts from background targets instead of cross sections

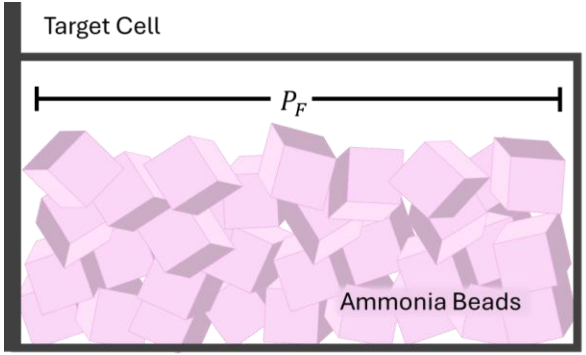

- $n_A \propto \sigma_{Al} + \sigma_{He} + \frac{7}{6}\sigma_C + \sigma_H$, where $\frac{7}{6}\sigma_C \approx \sigma_N$
- $n_{MT} \propto \sigma_{Al} + \sigma_{He}$
- $n_C \propto \sigma_{Al} + \sigma_{He} + \sigma_C$
- $n_{CH} \propto \sigma_{Al} + \sigma_{He} + \sigma_C + \sigma_H$
- $n_F \propto \sigma_{Al}$

- Solving for cross sections and rewriting the D_F yields

$$D_F(x, Q^2) = P_F \frac{C_1 n_C + C_2 n_{MT} + C_3 n_{CH} + C_4 n_F}{C_5 n_A}$$

- Packing fraction P_F is the target volume fraction occupied by the ammonia crystals

$$P_F(x, Q^2) = \frac{D_1(n_A - n_{MT})}{D_2 n_{MT} + D_3 n_C + D_4 n_{CH} + D_5 n_F}$$

$C_i, D_i \propto \ell_i, \rho_i$ of target materials

Calculating the Dilution Factor

- Two methods are used to calculate the dilution factor: a data-driven method and a model of the dilution factor

- Data-driven method:
  - Measure n_A n_{MT} n_C n_{CH} n_F from the data
  - Use these values to calculate a value of P_F for each x, Q^2 bin
  - Calculate a weighted average of all P_F
  - Use this $P_{F,avg}$ as an input to calculate D_F for each x, Q^2 bin
- Requires a radiation length correction to empty n_{MT} and foil n_F counts (haven't found a suitable model yet)

- Modeled dilution factor:
  - From modeled structure functions, "build" each target and simulate the counts n_A n_{MT} n_C n_{CH} n_F coming from the target
  - Allows for EMC effect, fermi motion, and radiative corrections to be built-in to the model
  - See Darren Upton's talk next for more details!
- Requires as an input values of P_F that must come from data

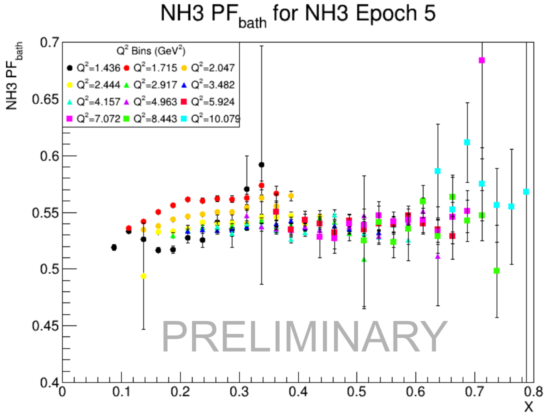

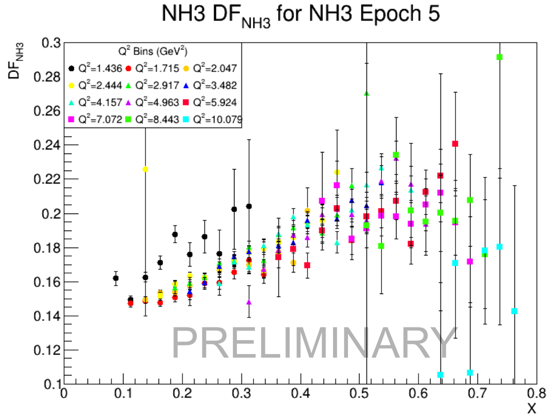

Preliminary Results

- Calculated preliminary D_F for the RGC dataset
- Datasets are broken up into different "epochs" that have different packing fraction
- D_F binned in x for each epoch
- Once D_F are calculated, use them to get $P_b P_t$

Summer 2022 Runs

Epoch 2: Runs 16137 – 16178
Epoch 3: Runs 16211 – 16260
Epoch 4: Runs 16318 – 16357
Epoch 5: Runs 16658 – 16695
Epoch 6: Runs 16709 – 16738
Epoch 7: Runs 16742 – 16772

Fall 2022 Runs

Epoch 8: Runs 16982 – 16995
Epoch 9: Runs 16996 – 17032
Epoch 10: Runs 17067 – 17102
Epoch 11: Runs 17144 – 17169
Epoch 12: Runs 17185 – 17225
Epoch 13: Runs 17353 – 17368
Epoch 14: Runs 17371 – 17382

Spring 2023 Runs

Epoch 15: Runs 17575 – 17597
Epoch 16: Runs 17598 – 17617
Epoch 17: Runs 17720 – 17741
Epoch 18: Runs 17748 – 17762

Summer 2022 D_F Data

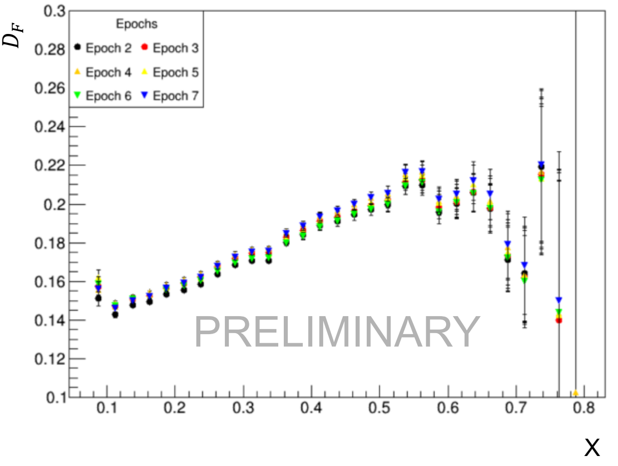

Fall 2022 D_F Data

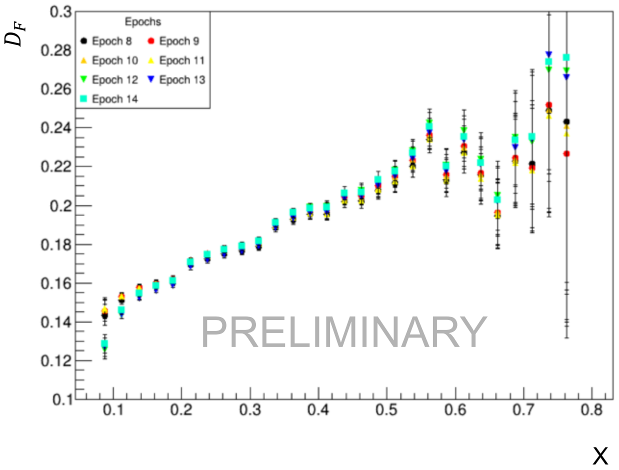

Spring 2023 D_F Data

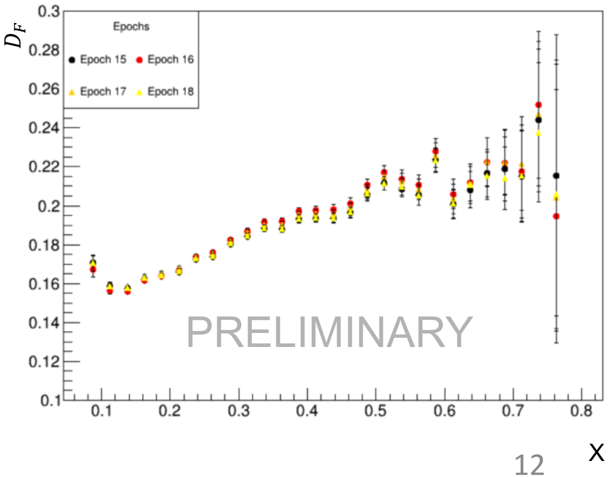

Preliminary Results

- Calculated preliminary D_F for the RGC dataset
- Datasets are broken up into different "epochs" that have different packing fraction
- D_F binned in x for each epoch
- Once D_F are calculated, use them to get $P_b P_t$

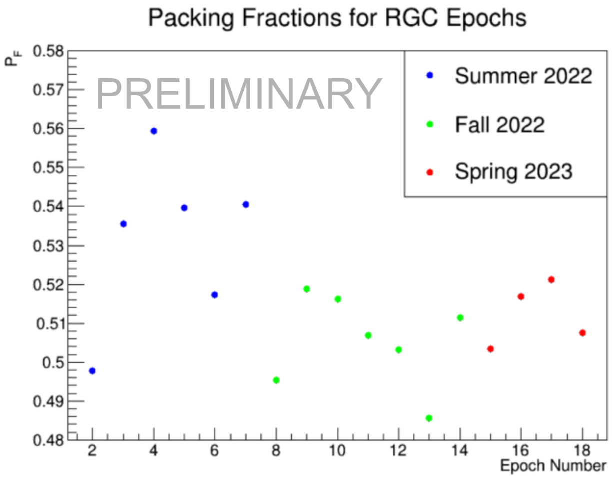

Summer 2022 D_F Data

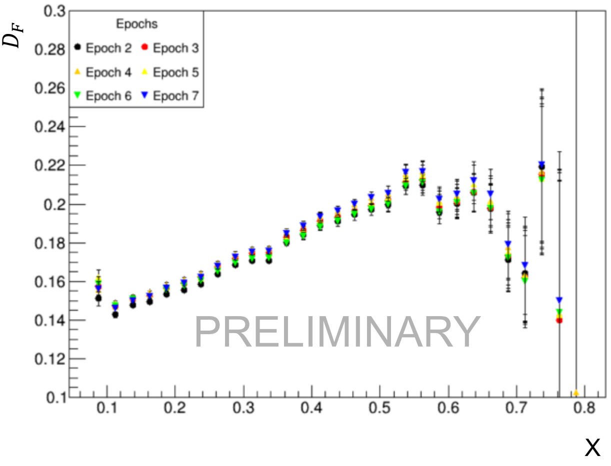

Fall 2022 D_F Data

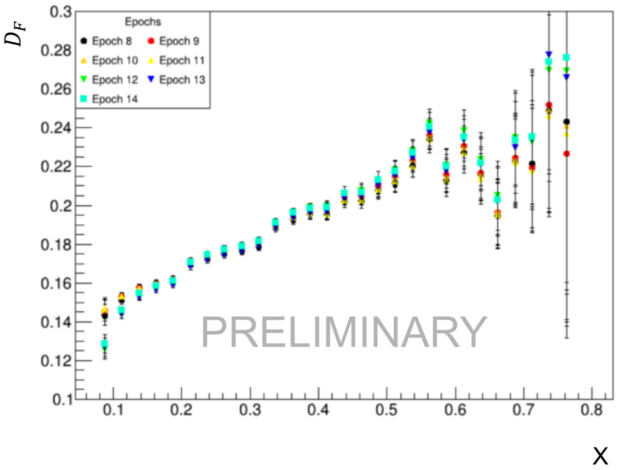

Spring 2023 D_F Data

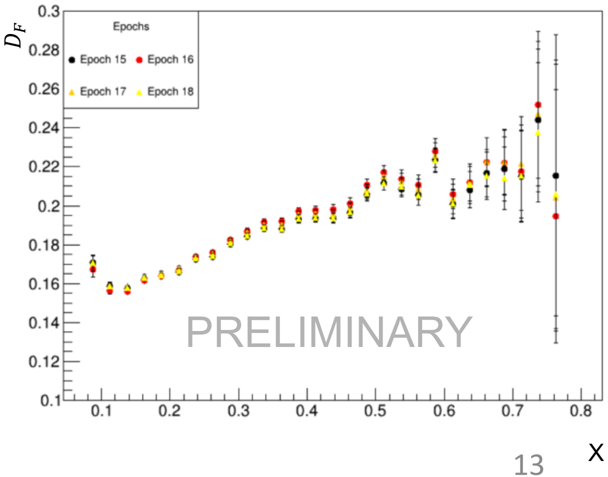

Beam-Target Polarization Calculations

$$A_{||,phys} = \frac{A_{||,raw}}{D_F P_b P_t} \quad \Rightarrow \quad P_b P_t = \frac{A_{||,raw}}{D_F A_{||,phys}}$$

- Use a model to calculate $A_{||,phys}$
- Values of $P_b P_t$ were calculated for RGC data using exclusive elastic $ep \rightarrow e'p'$ scattering (Noemie Pilleux)

$$P_b P_t = \frac{\sum_{Q^2\ bins} d_{f,i} A_{th,i} (n_i^- - n_i^+)}{\sum_{Q^2\ bins} d_{f,i}^2 A_{th,i}^2 (n_i^- + n_i^+)}$$

- d_f = separate dilution factor, A_{th} = elastic asymmetry parameterized by Arrington et. al.

- For DIS $P_b P_t$, calculated in x, Q^2 bins using $A_{th} = D(A_1 + \eta A_2)$, with Values of D, η, A_1, A_2 come from S. Kuhn 's model
- Much greater statistics than elastic

$$P_b P_t = \frac{\sum_{x,Q^2\ bins} D_{f,i} A_{th,i} (n_i^- - n_i^+)}{\sum_{x,Q^2\ bins} D_{f,i}^2 A_{th,i}^2 (n_i^- + n_i^+)}$$

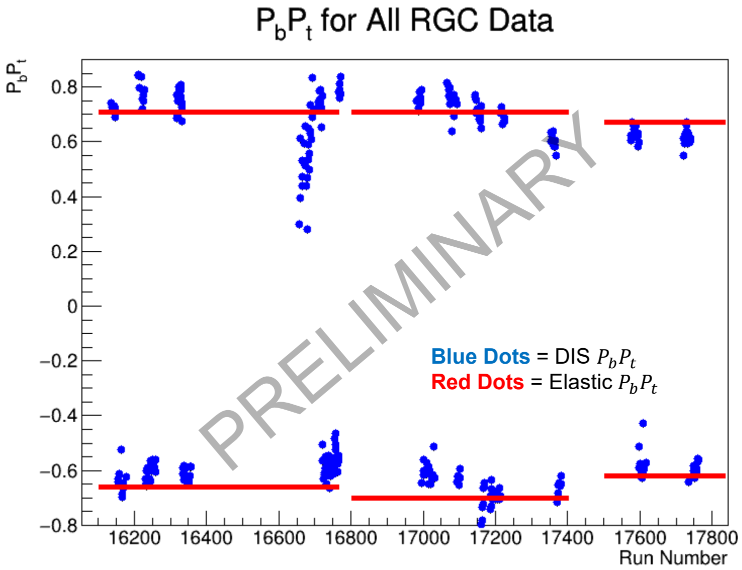

Normalize DIS $P_b P_t$ to elastic $P_b P_t$ to avoid circular calculation!

Preliminary Results

- To calculate $A_{1,p}$, rearrange $A_{||,phys} = D(A_1 + \eta A_2)$
- $A_1 = A_{||,phys}/D - \eta A_2$, with D, η, A_2 from S. Kuhn's model
- Values of η, A_2 are small for DIS kinematics, so smaller effects from model
- Spring 2023 data excludes outbending runs

- Data fluctuates around model values of $A_{1,p}$
- Slight dip at large x for Fall 2022 data

- Currently, we don't have data-driven $A_{1,d}$ results due to issues with calculating the ND3 D_F

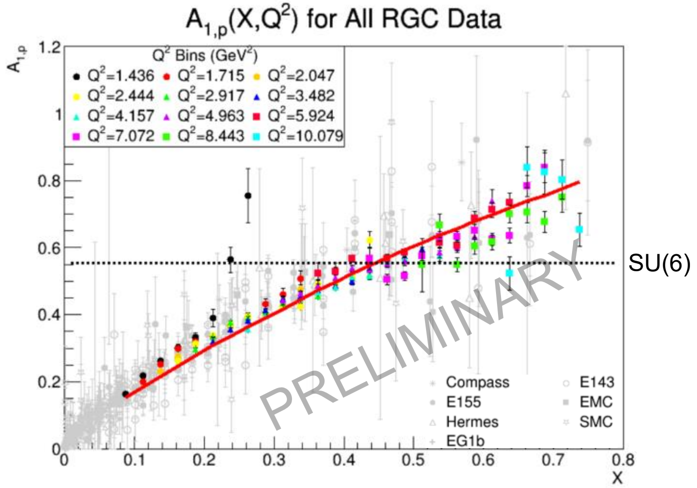

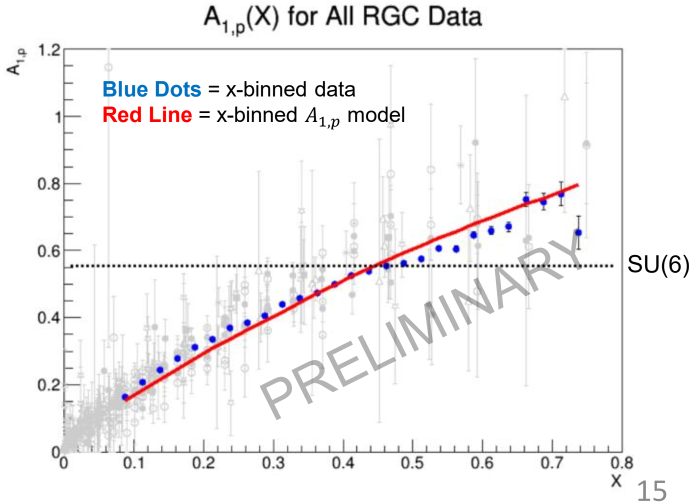

Preliminary Results

- To calculate $A_{1,p}$, rearrange $A_{||,phys} = D(A_1 + \eta A_2)$
- $A_1 = A_{||,phys}/D - \eta A_2$, with D, η, A_2 from S. Kuhn's model
- Values of η, A_2 are small for DIS kinematics, so smaller effects from model
- Spring 2023 data excludes outbending runs

- Data fluctuates around model values of $A_{1,p}$
- Slight dip at large x for Fall 2022 data

- Currently, we don't have data-driven $A_{1,d}$ results due to issues with calculating the ND3 D_F

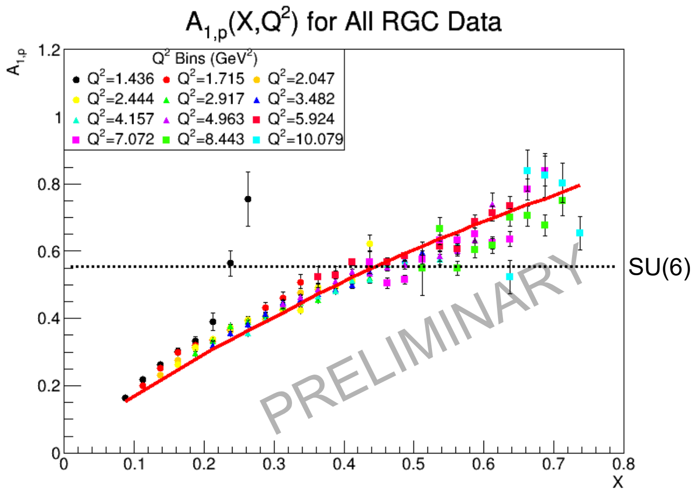

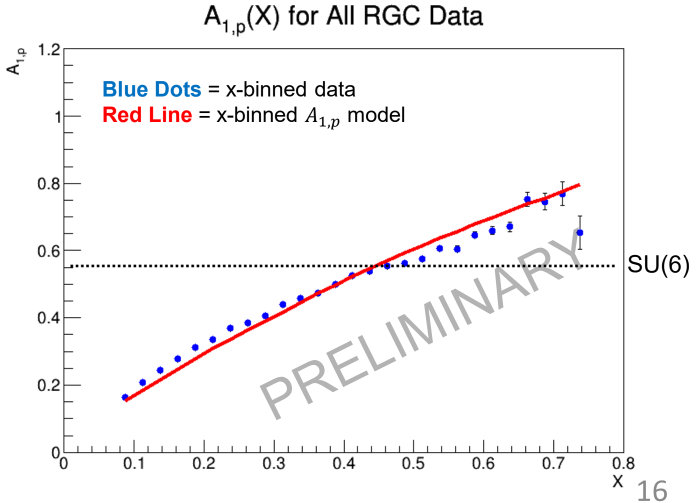

Preliminary Results

- To calculate $A_{1,p}$, rearrange $A_{||,phys} = D(A_1 + \eta A_2)$
- $A_1 = A_{||,phys}/D - \eta A_2$, with D, η, A_2 from S. Kuhn's model
- Values of η, A_2 are small for DIS kinematics, so smaller effects from model
- Spring 2023 data excludes outbending runs

- Data fluctuates around model values of $A_{1,p}$
- Slight dip at large x for Fall 2022 data

- Currently, we don't have data-driven $A_{1,d}$ results due to issues with calculating the ND3 D_F

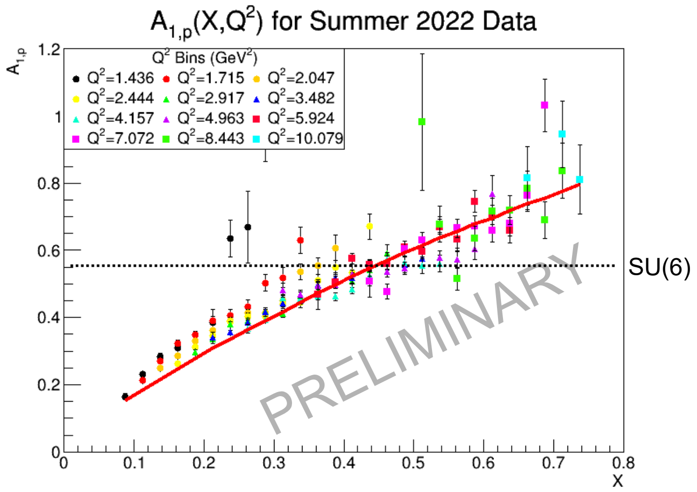

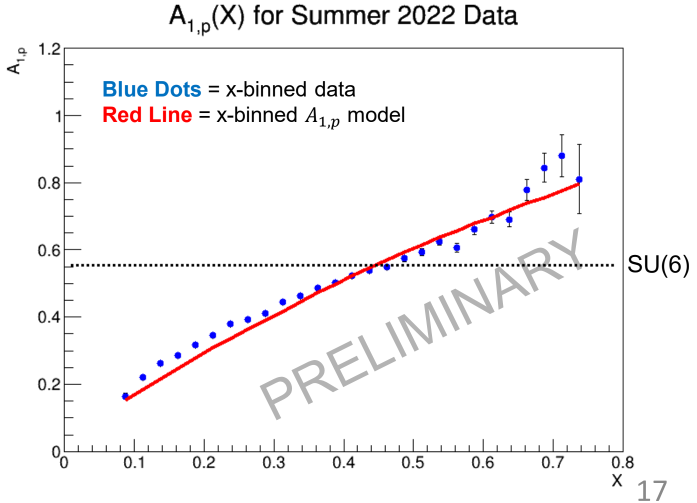

Preliminary Results

- To calculate $A_{1,p}$, rearrange $A_{||,phys} = D(A_1 + \eta A_2)$
- $A_1 = A_{||,phys}/D - \eta A_2$, with D, η, A_2 from S. Kuhn's model
- Values of η, A_2 are small for DIS kinematics, so smaller effects from model
- Spring 2023 data excludes outbending runs

- Data fluctuates around model values of $A_{1,p}$
- Slight dip at large x for Fall 2022 data

- Currently, we don't have data-driven $A_{1,d}$ results due to issues with calculating the ND3 D_F

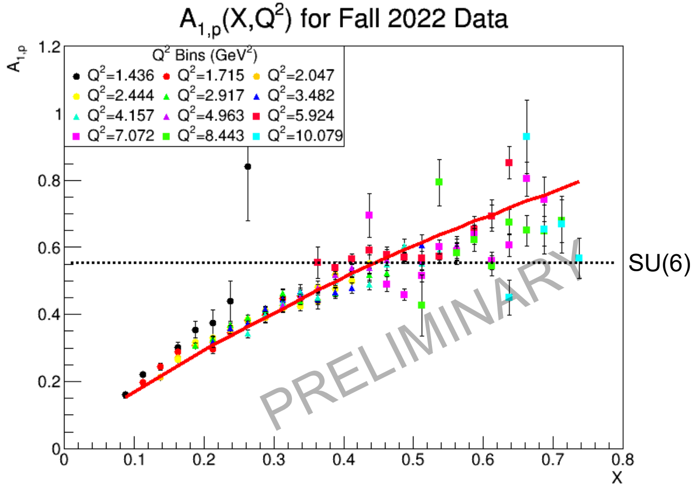

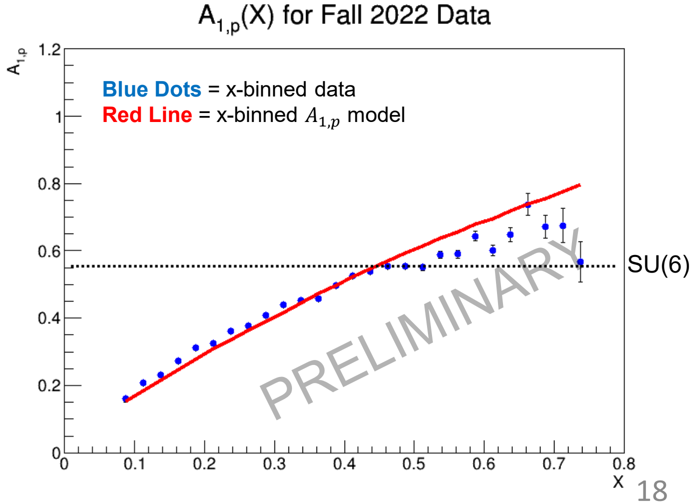

Preliminary Results

- To calculate $A_{1,p}$, rearrange $A_{||,phys} = D(A_1 + \eta A_2)$
- $A_1 = A_{||,phys}/D - \eta A_2$, with D, η, A_2 from S. Kuhn's model
- Values of η, A_2 are small for DIS kinematics, so smaller effects from model
- Spring 2023 data excludes outbending runs

- Data fluctuates around model values of $A_{1,p}$
- Slight dip at large x for Fall 2022 data

- Currently, we don't have data-driven $A_{1,d}$ results due to issues with calculating the ND3 D_F

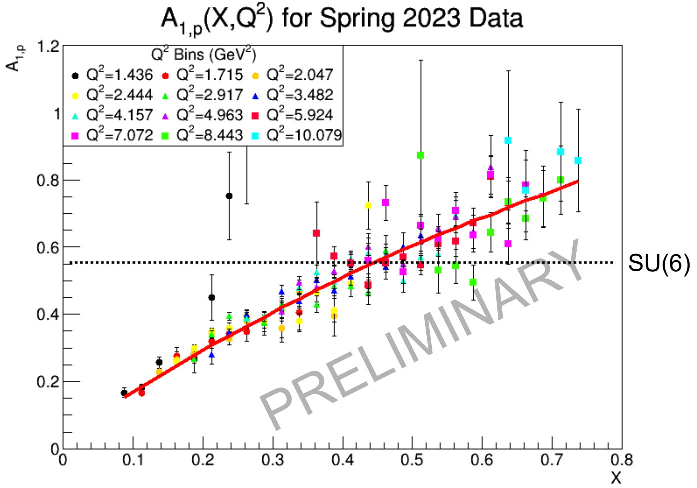

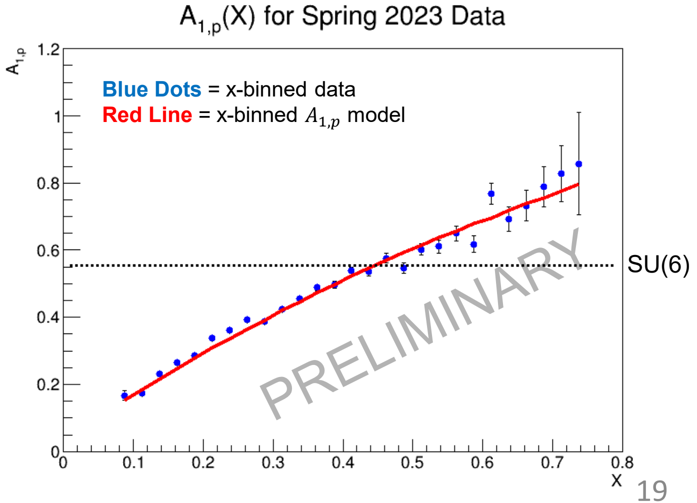

Work Left To Do

- Study accuracy of thermal contractions applied to target geometries
- Incorporate radiation length corrections to $n_{MT}, \ n_F$ counts
- Subtract background from misidentified π^-, e^+e^- pair production
- Correct $P_b P_t$ for polarized ^{14}N in target
- Figure out why low Q^2 looks so rough

- Finalize the D_F model-driven approach

- Fiducial Cuts
  - Cuts on DC hit position (either local $\theta, \ \phi$ variables and/or edge variable cuts)
  - Cuts on ECAL hit position and sampling fraction values

- Any Questions?

Backup Slides

- Thermal expansion corrections to targets
- Data Quality Per Q^2 Bin
- All D_F and P_F for NH3 targets across all x, Q^2 bins
- All D_F and P_F for ND3 targets across all x, Q^2 bins

Thermal Contraction of Targets

- Studying the impact of thermal contraction of the target cells on the dilution factor
- Carbon, CH2, CD2 targets' geometry measured at room temperature, cooled to ~1K, so there's some contraction of target length
- Modulate the sizes of the targets as follows:
  - $\ell_C * (1 - dL_C/L_C)$, with dL_C/L_C = 0.5%
  - $\ell_{CH} * (1 - dL_{CH}/L_{CH})$, with dL_{CH}/L_{CH} = 2.1%
  - $\ell_{CD} * (1 - dL_{CH}/L_{CH})$
  - $L * (1 - 0.018)$ (for Teflon contraction, 1.8%)
  - $\rho_C/(1 - dL_{CH}/L_{CH})^3$
  - $\rho_{CH}\ /(1 - dL_{CH}/L_{CH})^3$
  - $\rho_{CD}/(1 - dL_{CH}/L_{CH})^3$
  - ρ_A, ρ_D are unchanged

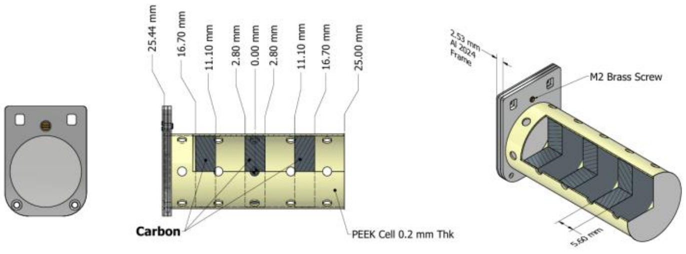

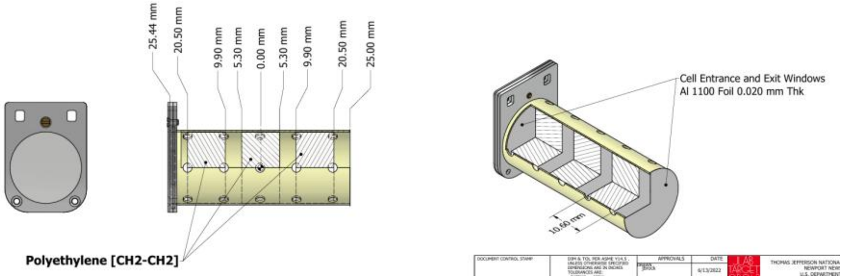

Calculating the Dilution Factor

- Advantageous to write D_F in terms of scattering counts from background targets instead of cross sections

- $n_A \propto \sigma_{Al}\ell_{Al}\rho_{Al} + \sigma_{He}(L-\ell_A)\rho_{He} + \left(\frac{7}{6}\sigma_C + 3\sigma_H\right)\ell_A\rho_A$
- $n_{MT} \propto \sigma_{Al}\ell_{Al}\rho_{Al} + \sigma_{He}L\rho_{He}$
- $n_C \propto \sigma_{Al}\ell_{Al}\rho_{Al} + \sigma_{He}(L-\ell_C)\rho_{He} + \sigma_C\ell_C\rho_C$
- $n_{CH} \propto \sigma_{Al}\ell_{Al}\rho_{Al} + \sigma_{He}(L-\ell_{CH})\rho_{He} + (\sigma_C + 2\sigma_H)\ell_{CH}\rho_{CH}$
- $n_F \propto \sigma_{Al}\ell_{Al}\rho_{Al}$

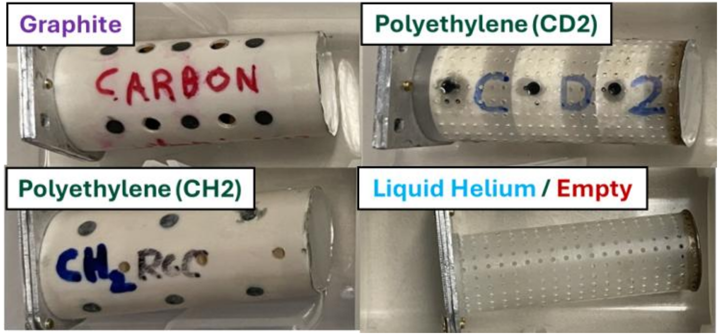

- Solving for cross sections and rewriting the D_F yields

$$D_F(x,Q^2) = P_F\frac{3\rho_A}{2n_A\rho_C\rho_{CH}}\left(\frac{L}{\ell_{CH}}\rho_C(n_{CH}-n_{MT}) + (\rho_C-\rho_{CH})(n_{MT}-n_F) - \frac{L}{\ell_C}\rho_{CH}(n_C-n_{MT})\right)$$

- Packing fraction P_F is the target volume fraction occupied by the ammonia crystals

$$P_F(x,Q^2) = \frac{6\ell_C\rho_C\ell_{CH}\rho_{CH}(n_A-n_{MT})}{2\ell_{CH}\rho_{CH}L\rho_A(n_{MT}-n_C) + 9\ell_C\rho_C L\rho_A(n_{CH}-n_{MT}) + \ell_C\ell_{CH}(n_{MT}-n_F)(9\rho_A\rho_C - 2(\rho_A+3\rho_C)\rho_{CH})}$$

Calculating the Dilution Factor

- Advantageous to write D_F in terms of scattering counts from background targets instead of cross sections

- $n_A \propto \sigma_{Al}\ell_{Al}\rho_{Al} + \sigma_{He}(L - \ell_A)\rho_{He} + \left(\frac{7}{6}\sigma_C + 3\sigma_H\right)\ell_A\rho_A$
- $n_{MT} \propto \sigma_{Al}\ell_{Al}\rho_{Al} + \sigma_{He}L\rho_{He}$
- $n_C \propto \sigma_{Al}\ell_{Al}\rho_{Al} + \sigma_{He}(L - \ell_C)\rho_{He} + \sigma_C\ell_C\rho_C$
- $n_{CH} \propto \sigma_{Al}\ell_{Al}\rho_{Al} + \sigma_{He}(L - \ell_{CH})\rho_{He} + (\sigma_C + 2\sigma_H)\ell_{CH}\rho_{CH}$
- $n_F \propto \sigma_{Al}\ell_{Al}\rho_{Al}$

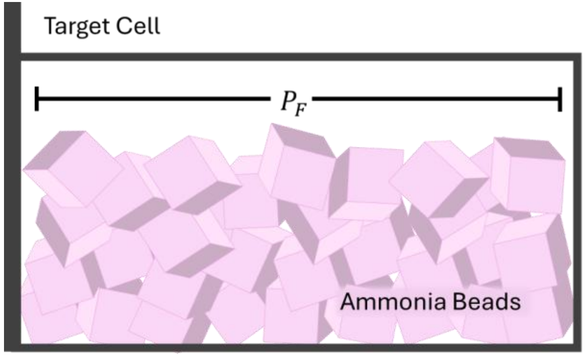

- Solving for cross sections and rewriting the D_F yields

$$D_F(x, Q^2) = P_F \frac{3\rho_A}{2n_A\rho_C\rho_{CH}}\left(\frac{L}{\ell_{CH}}\rho_C(n_{CH} - n_{MT}) + (\rho_C - \rho_{CH})(n_{MT} - n_F) - \frac{L}{\ell_C}\rho_{CH}(n_C - n_{MT})\right)$$

- Packing fraction P_F is the target volume fraction occupied by the ammonia crystals

$$P_F(x, Q^2) = \frac{6\ell_C\rho_C\ell_{CH}\rho_{CH}(n_A - n_{MT})}{2\ell_{CH}\rho_{CH}L\rho_A(n_{MT} - n_C) + 9\ell_C\rho_C L\rho_A(n_{CH} - n_{MT}) + \ell_C\ell_{CH}(n_{MT} - n_F)(9\rho_A\rho_C - 2(\rho_A + 3\rho_C)\rho_{CH})}$$

Data Quality Per Q^2 Bin

- Issue with CLAS12 data: inconsistent behavior of D_F, P_F in low Q^2 bins of data
- Plotted DC hit position, χ^2_{track}/NDF vs. edge, θ distributions for each bin in Q^2

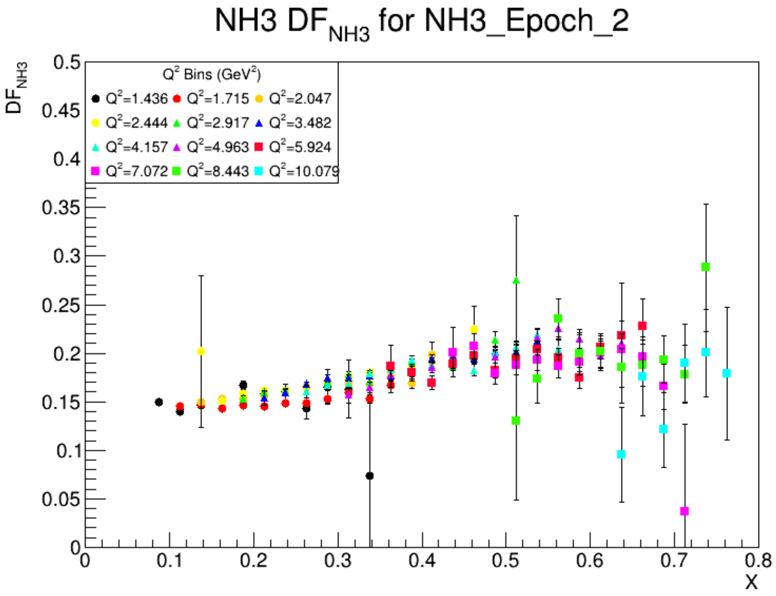

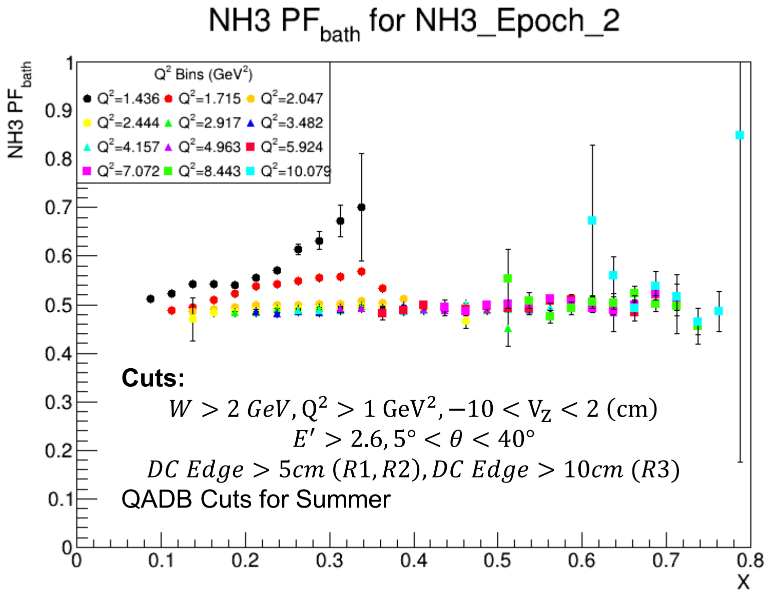

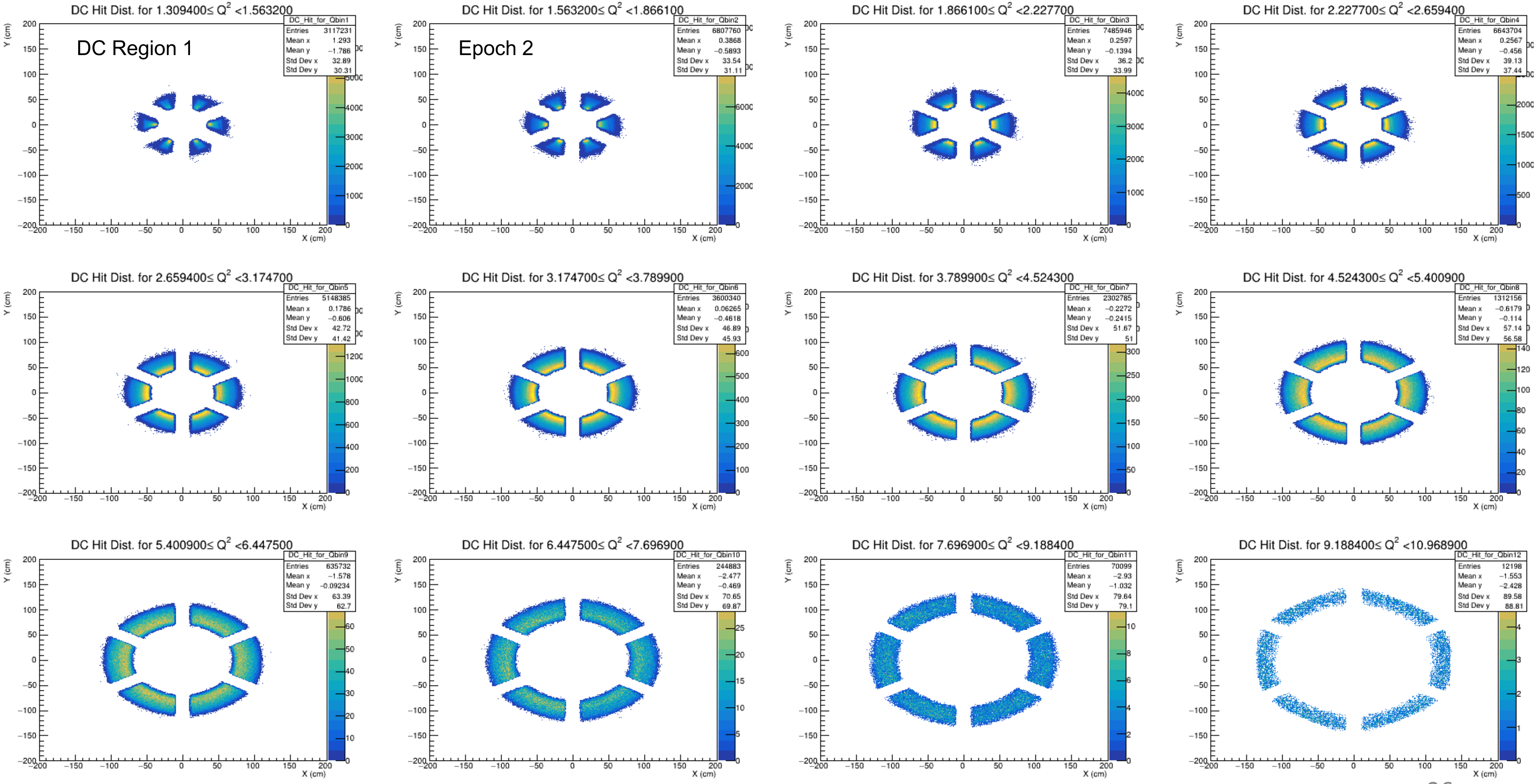
DC Region 1
Epoch 2
DC Hit Dist. for 1.309400≤ Q² <1.563200
DC_Hit_for_Qbin1 Entries 3117231 Mean x 1.293 Mean y −1.786 Std Dev x 32.89 Std Dev y 30.31
DC Hit Dist. for 1.563200≤ Q² <1.866100
DC_Hit_for_Qbin2 Entries 6807760 Mean x 0.3868 Mean y −0.5893 Std Dev x 33.54 Std Dev y 31.11
DC Hit Dist. for 1.866100≤ Q² <2.227700
DC_Hit_for_Qbin3 Entries 7485946 Mean x 0.2597 Mean y −0.1394 Std Dev x 36.2 Std Dev y 33.99
DC Hit Dist. for 2.227700≤ Q² <2.659400
DC_Hit_for_Qbin4 Entries 6643704 Mean x 0.2567 Mean y −0.456 Std Dev x 39.13 Std Dev y 37.44
DC Hit Dist. for 2.659400≤ Q² <3.174700
DC_Hit_for_Qbin5 Entries 5148385 Mean x 0.1786 Mean y −0.606 Std Dev x 42.72 Std Dev y 41.42
DC Hit Dist. for 3.174700≤ Q² <3.789900
DC_Hit_for_Qbin6 Entries 3600340 Mean x 0.06265 Mean y −0.4618 Std Dev x 46.89 Std Dev y 45.93
DC Hit Dist. for 3.789900≤ Q² <4.524300
DC_Hit_for_Qbin7 Entries 2302785 Mean x −0.2272 Mean y −0.2415 Std Dev x 51.67 Std Dev y 51
DC Hit Dist. for 4.524300≤ Q² <5.400900
DC_Hit_for_Qbin8 Entries 1312156 Mean x −0.6179 Mean y −0.114 Std Dev x 57.14 Std Dev y 56.58
DC Hit Dist. for 5.400900≤ Q² <6.447500
DC_Hit_for_Qbin9 Entries 635732 Mean x −1.578 Mean y −0.09234 Std Dev x 63.39 Std Dev y 62.7
DC Hit Dist. for 6.447500≤ Q² <7.696900
DC_Hit_for_Qbin10 Entries 244883 Mean x −2.477 Mean y −0.469 Std Dev x 70.65 Std Dev y 69.87
DC Hit Dist. for 7.696900≤ Q² <9.188400
DC_Hit_for_Qbin11 Entries 70099 Mean x −2.93 Mean y −1.032 Std Dev x 79.64 Std Dev y 79.1
DC Hit Dist. for 9.188400≤ Q² <10.968900
DC_Hit_for_Qbin12 Entries 12198 Mean x −1.553 Mean y −2.428 Std Dev x 89.58 Std Dev y 88.81
X (cm)
Y (cm)

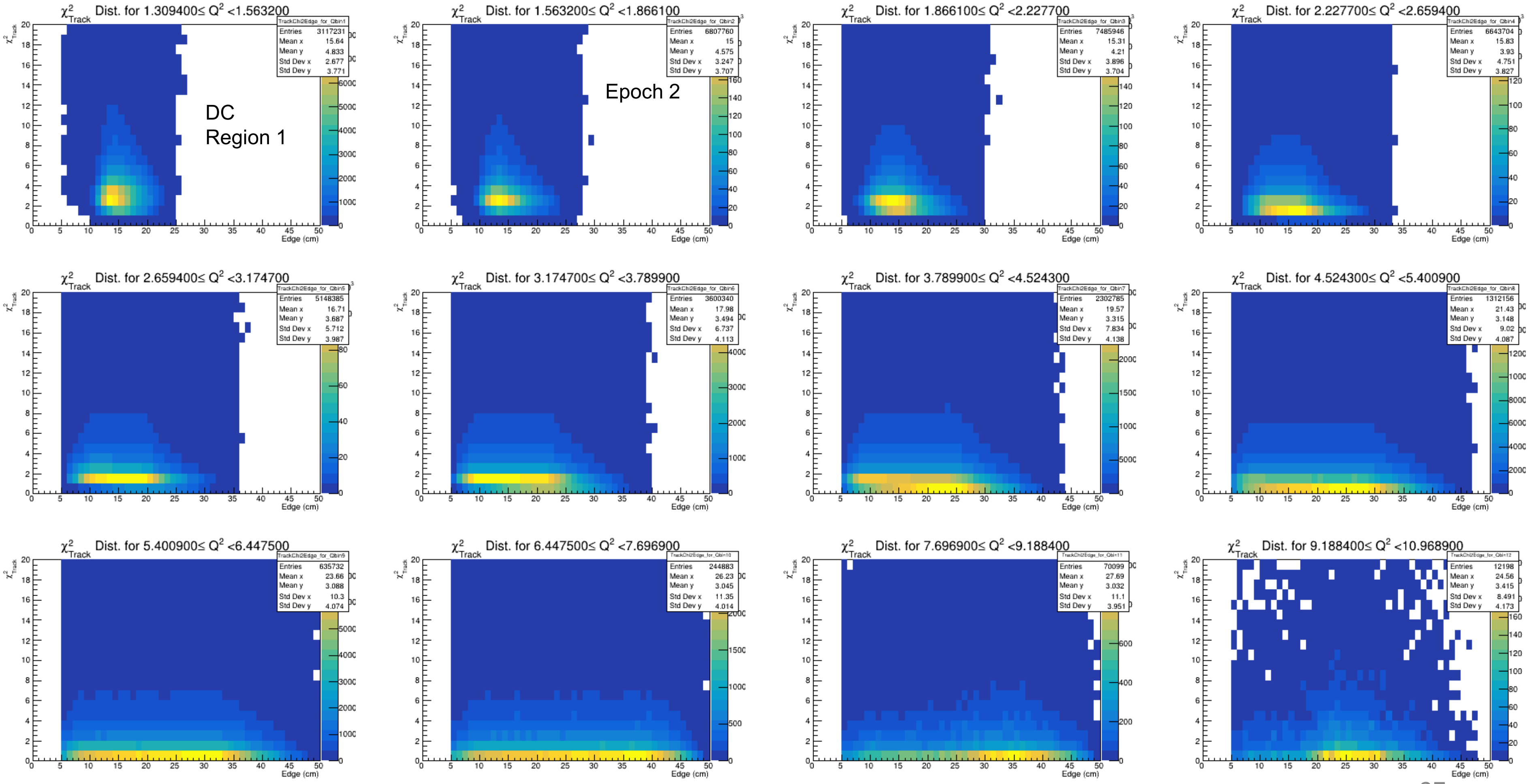
DC
Region 1
Epoch 2
χ²Track Dist. for 1.309400≤ Q² <1.563200
Entries 3117231 Mean x 15.64 Mean y 4.833 Std Dev x 2.677 Std Dev y 3.771
χ²Track Dist. for 1.563200≤ Q² <1.866100
Entries 6807760 Mean x 15 Mean y 4.575 Std Dev x 3.247 Std Dev y 3.707
χ²Track Dist. for 1.866100≤ Q² <2.227700
Entries 7485946 Mean x 15.31 Mean y 4.21 Std Dev x 3.896 Std Dev y 3.704
χ²Track Dist. for 2.227700≤ Q² <2.659400
Entries 6643704 Mean x 15.83 Mean y 3.93 Std Dev x 4.751 Std Dev y 3.827
χ²Track Dist. for 2.659400≤ Q² <3.174700
Entries 5148385 Mean x 16.71 Mean y 3.687 Std Dev x 5.712 Std Dev y 3.987
χ²Track Dist. for 3.174700≤ Q² <3.789900
Entries 3600340 Mean x 17.98 Mean y 3.494 Std Dev x 6.737 Std Dev y 4.113
χ²Track Dist. for 3.789900≤ Q² <4.524300
Entries 2302785 Mean x 19.57 Mean y 3.315 Std Dev x 7.834 Std Dev y 4.138
χ²Track Dist. for 4.524300≤ Q² <5.400900
Entries 1312156 Mean x 21.43 Mean y 3.148 Std Dev x 9.02 Std Dev y 4.087
χ²Track Dist. for 5.400900≤ Q² <6.447500
Entries 635732 Mean x 23.66 Mean y 3.088 Std Dev x 10.3 Std Dev y 4.074
χ²Track Dist. for 6.447500≤ Q² <7.696900
Entries 244883 Mean x 26.23 Mean y 3.045 Std Dev x 11.35 Std Dev y 4.014
χ²Track Dist. for 7.696900≤ Q² <9.188400
Entries 70099 Mean x 27.69 Mean y 3.032 Std Dev x 11.1 Std Dev y 3.951
χ²Track Dist. for 9.188400≤ Q² <10.968900
Entries 12198 Mean x 24.56 Mean y 3.415 Std Dev x 8.491 Std Dev y 4.173
Edge (cm)

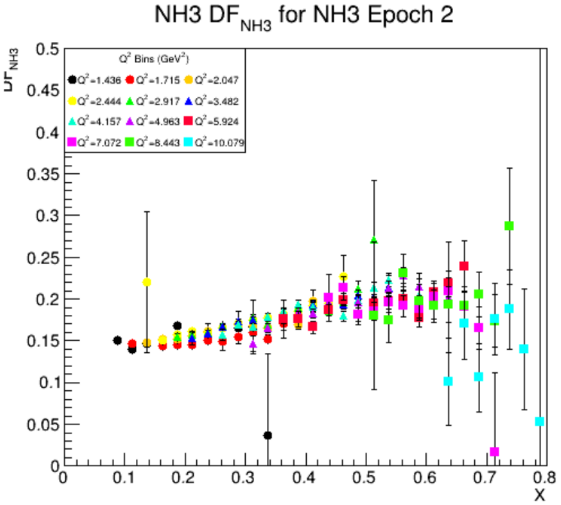

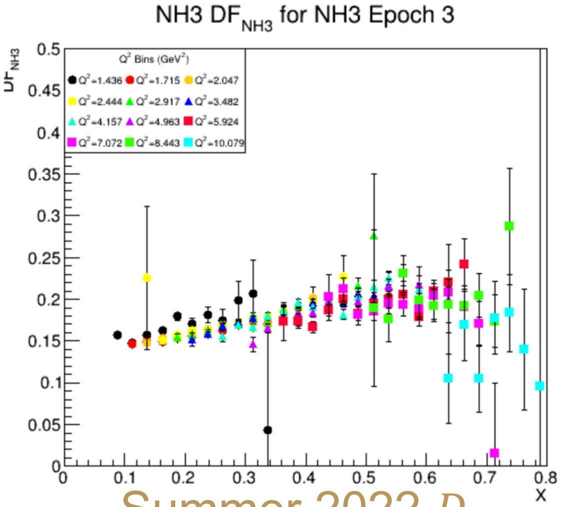

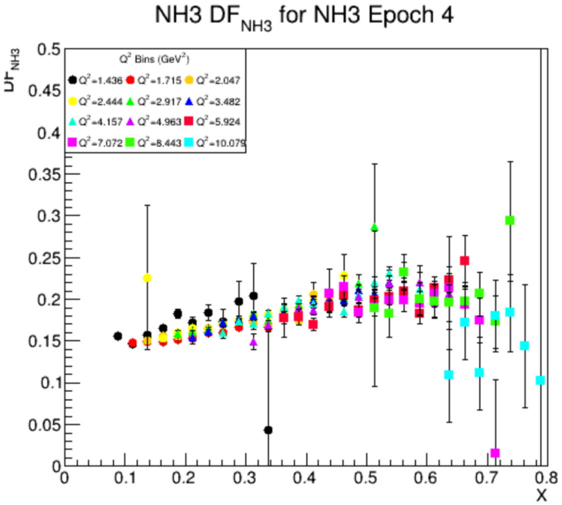

Summer 2022 D_F

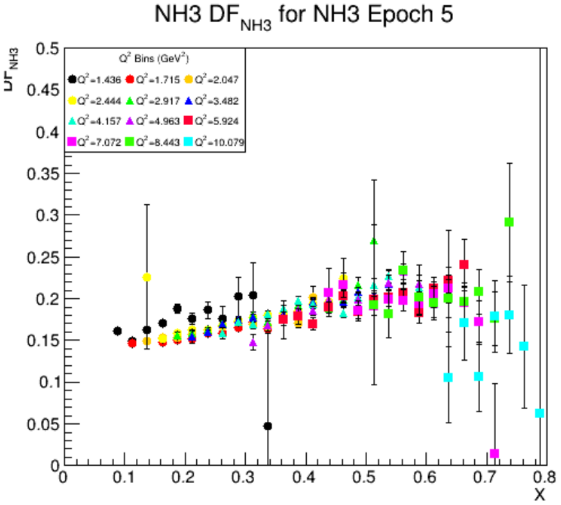

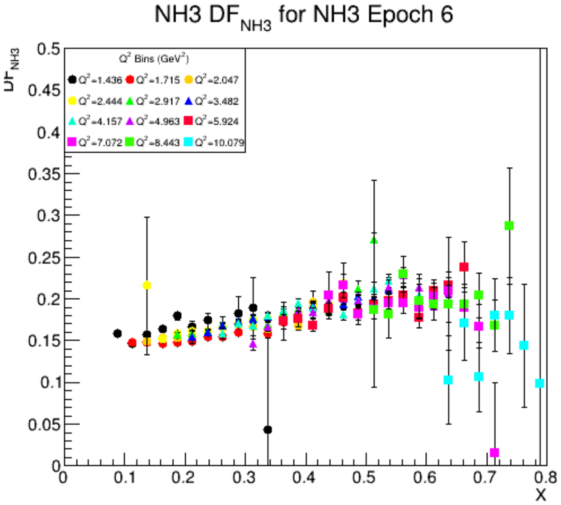

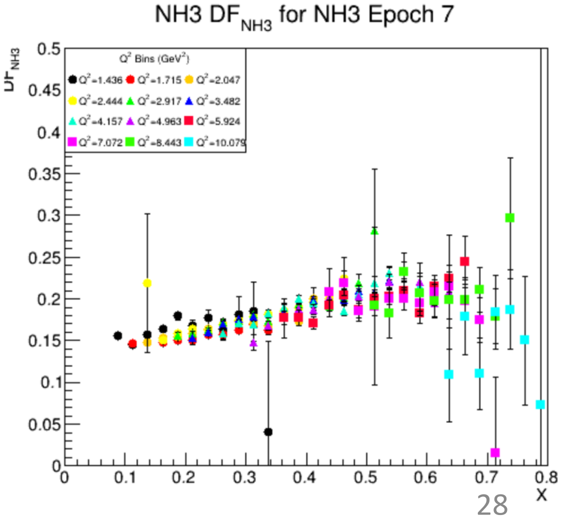

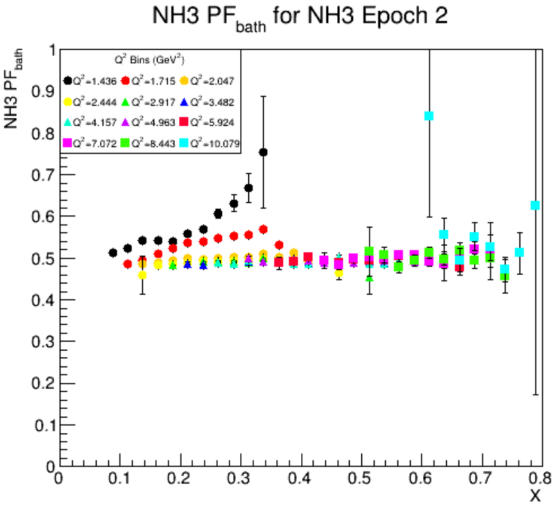

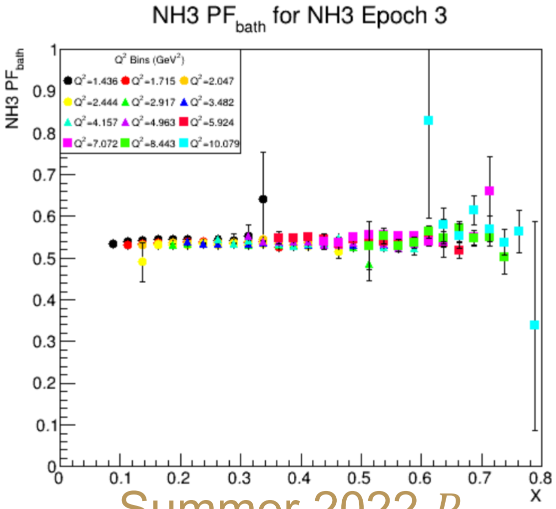

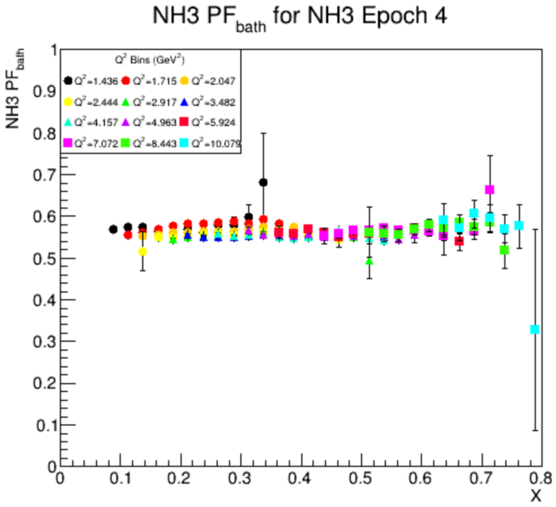

Summer 2022 P_F

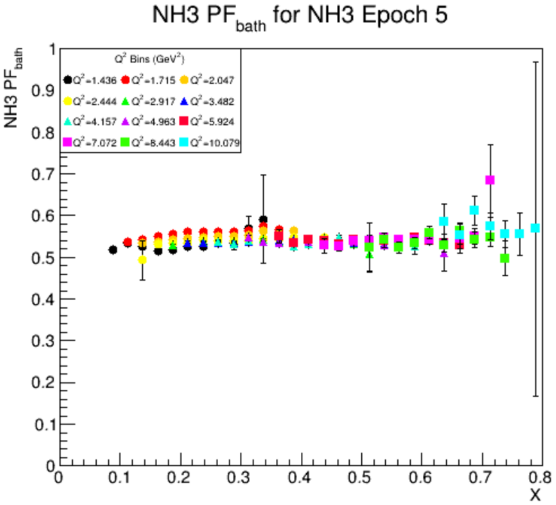

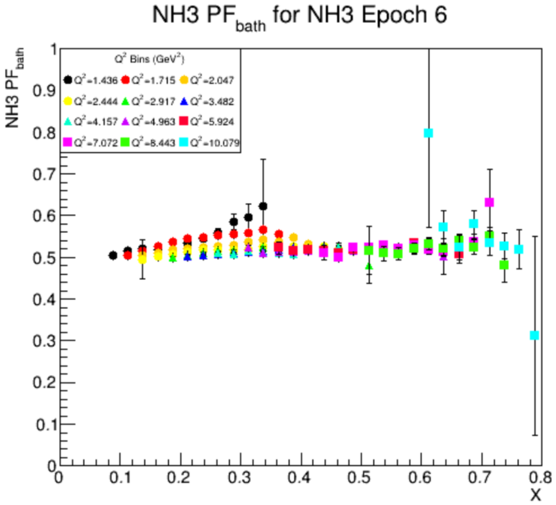

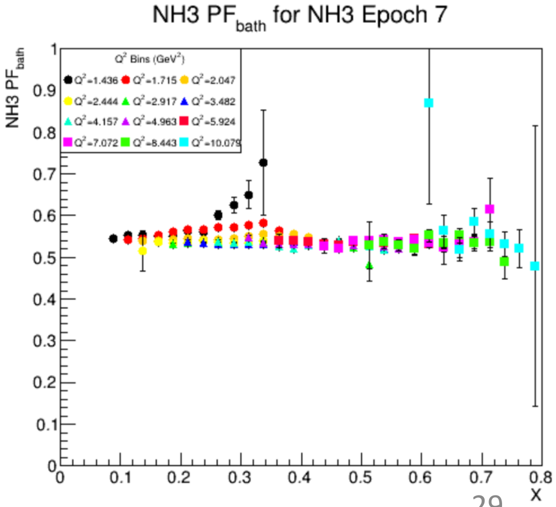

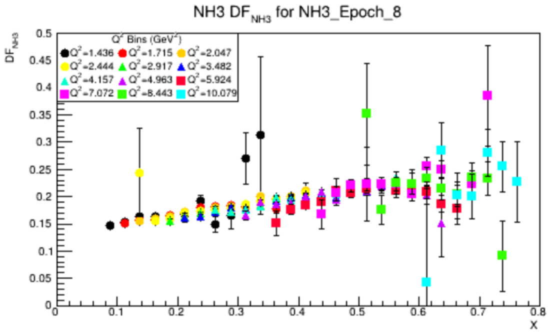
NH3 DF_NH3 for NH3_Epoch_8
Q² Bins (GeV²)
Q²=1.436 Q²=1.715 Q²=2.047
Q²=2.444 Q²=2.917 Q²=3.482
Q²=4.157 Q²=4.963 Q²=5.924
Q²=7.072 Q²=8.443 Q²=10.079
DF_NH3
x

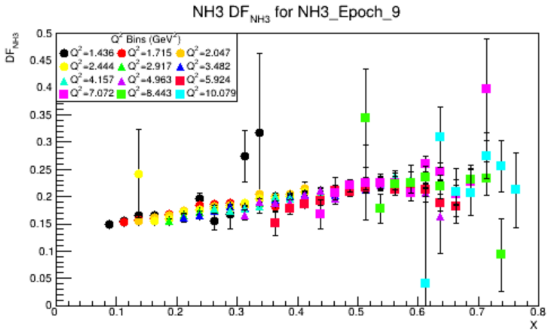
NH3 DF_NH3 for NH3_Epoch_9
Q² Bins (GeV²)
Q²=1.436 Q²=1.715 Q²=2.047
Q²=2.444 Q²=2.917 Q²=3.482
Q²=4.157 Q²=4.963 Q²=5.924
Q²=7.072 Q²=8.443 Q²=10.079
DF_NH3
x

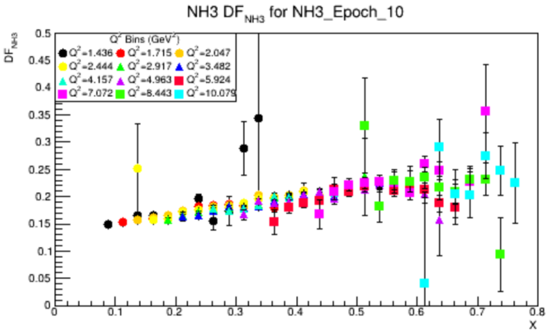
NH3 DF_NH3 for NH3_Epoch_10
Q² Bins (GeV²)
Q²=1.436 Q²=1.715 Q²=2.047
Q²=2.444 Q²=2.917 Q²=3.482
Q²=4.157 Q²=4.963 Q²=5.924
Q²=7.072 Q²=8.443 Q²=10.079
DF_NH3
x

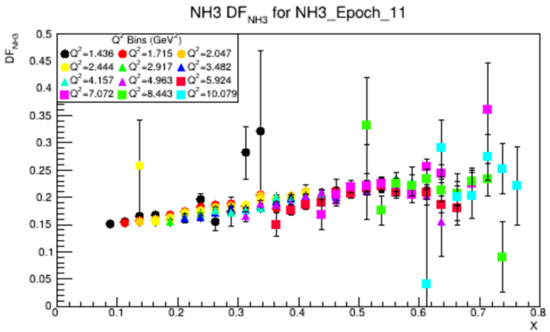
NH3 DF_NH3 for NH3_Epoch_11
Q² Bins (GeV²)
Q²=1.436 Q²=1.715 Q²=2.047
Q²=2.444 Q²=2.917 Q²=3.482
Q²=4.157 Q²=4.963 Q²=5.924
Q²=7.072 Q²=8.443 Q²=10.079
DF_NH3
x

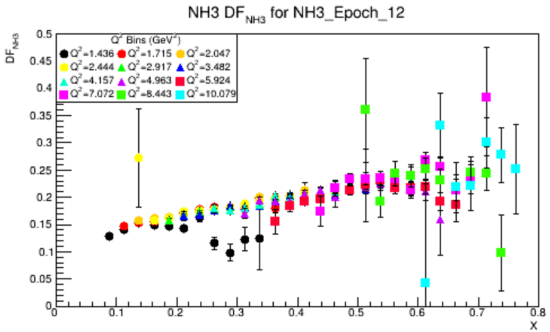
NH3 DF_NH3 for NH3_Epoch_12
Q² Bins (GeV²)
Q²=1.436 Q²=1.715 Q²=2.047
Q²=2.444 Q²=2.917 Q²=3.482
Q²=4.157 Q²=4.963 Q²=5.924
Q²=7.072 Q²=8.443 Q²=10.079
DF_NH3
x

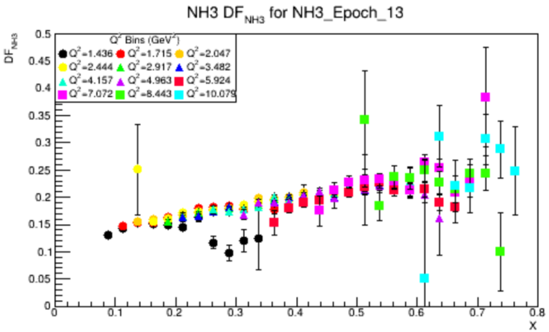
NH3 DF_NH3 for NH3_Epoch_13
Q² Bins (GeV²)
Q²=1.436 Q²=1.715 Q²=2.047
Q²=2.444 Q²=2.917 Q²=3.482
Q²=4.157 Q²=4.963 Q²=5.924
Q²=7.072 Q²=8.443 Q²=10.079
DF_NH3
x

Fall 2022 D_F

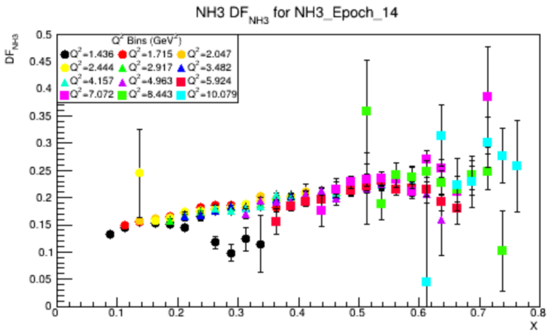
NH3 DF_NH3 for NH3_Epoch_14
Q² Bins (GeV²)
Q²=1.436 Q²=1.715 Q²=2.047
Q²=2.444 Q²=2.917 Q²=3.482
Q²=4.157 Q²=4.963 Q²=5.924
Q²=7.072 Q²=8.443 Q²=10.079
DF_NH3
x

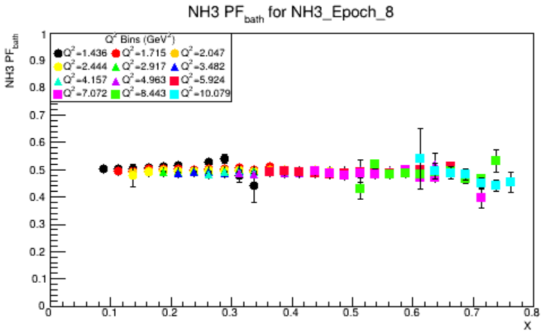
NH3 PF_bath for NH3_Epoch_8
NH3 PF_bath
x
Q^2 Bins (GeV^2)
Q^2=1.436 Q^2=1.715 Q^2=2.047
Q^2=2.444 Q^2=2.917 Q^2=3.482
Q^2=4.157 Q^2=4.963 Q^2=5.924
Q^2=7.072 Q^2=8.443 Q^2=10.079

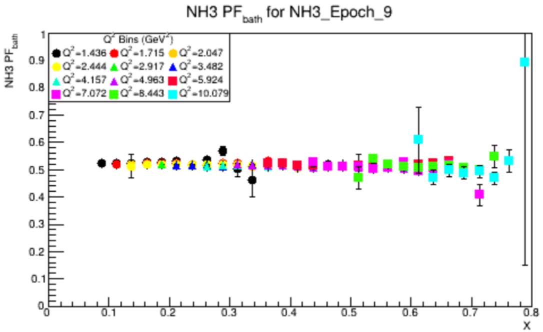
NH3 PF_bath for NH3_Epoch_9
NH3 PF_bath
x
Q^2 Bins (GeV^2)
Q^2=1.436 Q^2=1.715 Q^2=2.047
Q^2=2.444 Q^2=2.917 Q^2=3.482
Q^2=4.157 Q^2=4.963 Q^2=5.924
Q^2=7.072 Q^2=8.443 Q^2=10.079

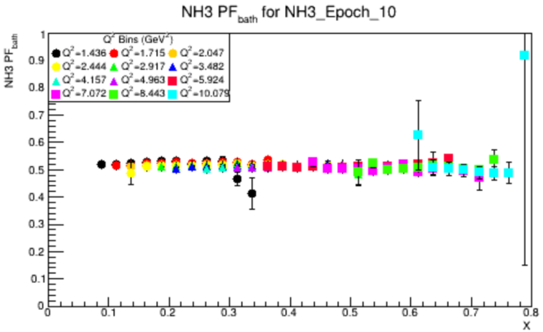
NH3 PF_bath for NH3_Epoch_10
NH3 PF_bath
x
Q^2 Bins (GeV^2)
Q^2=1.436 Q^2=1.715 Q^2=2.047
Q^2=2.444 Q^2=2.917 Q^2=3.482
Q^2=4.157 Q^2=4.963 Q^2=5.924
Q^2=7.072 Q^2=8.443 Q^2=10.079

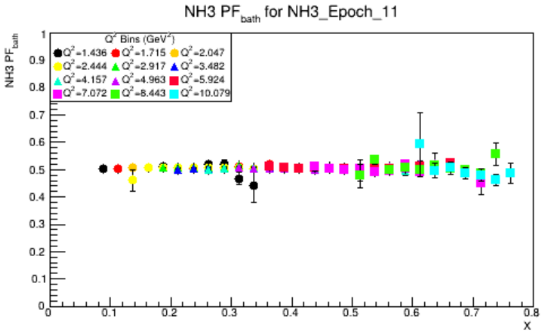
NH3 PF_bath for NH3_Epoch_11
NH3 PF_bath
x
Q^2 Bins (GeV^2)
Q^2=1.436 Q^2=1.715 Q^2=2.047
Q^2=2.444 Q^2=2.917 Q^2=3.482
Q^2=4.157 Q^2=4.963 Q^2=5.924
Q^2=7.072 Q^2=8.443 Q^2=10.079

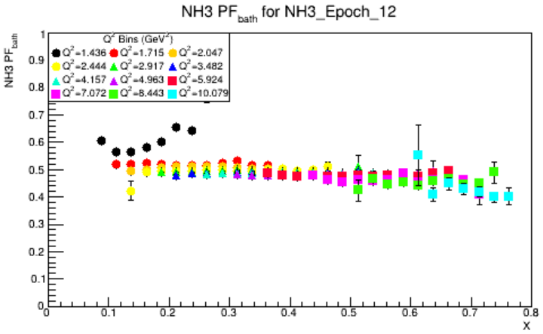
NH3 PF_bath for NH3_Epoch_12
NH3 PF_bath
x
Q^2 Bins (GeV^2)
Q^2=1.436 Q^2=1.715 Q^2=2.047
Q^2=2.444 Q^2=2.917 Q^2=3.482
Q^2=4.157 Q^2=4.963 Q^2=5.924
Q^2=7.072 Q^2=8.443 Q^2=10.079

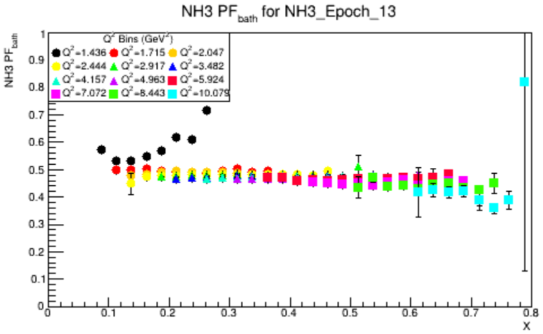
NH3 PF_bath for NH3_Epoch_13
NH3 PF_bath
x
Q^2 Bins (GeV^2)
Q^2=1.436 Q^2=1.715 Q^2=2.047
Q^2=2.444 Q^2=2.917 Q^2=3.482
Q^2=4.157 Q^2=4.963 Q^2=5.924
Q^2=7.072 Q^2=8.443 Q^2=10.079

Fall 2022 P_F

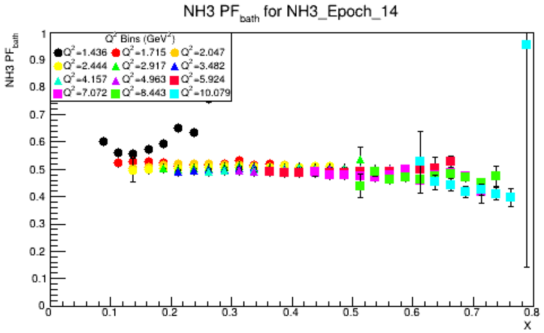
NH3 PF_bath for NH3_Epoch_14
NH3 PF_bath
x
Q^2 Bins (GeV^2)
Q^2=1.436 Q^2=1.715 Q^2=2.047
Q^2=2.444 Q^2=2.917 Q^2=3.482
Q^2=4.157 Q^2=4.963 Q^2=5.924
Q^2=7.072 Q^2=8.443 Q^2=10.079

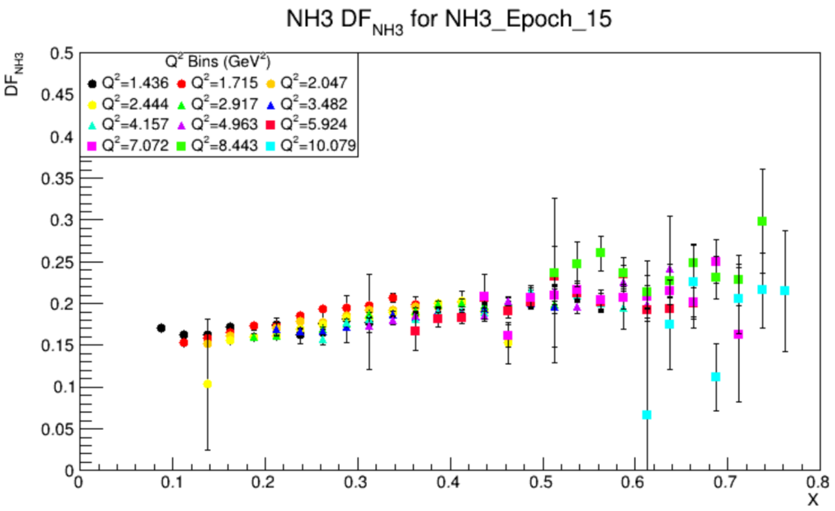

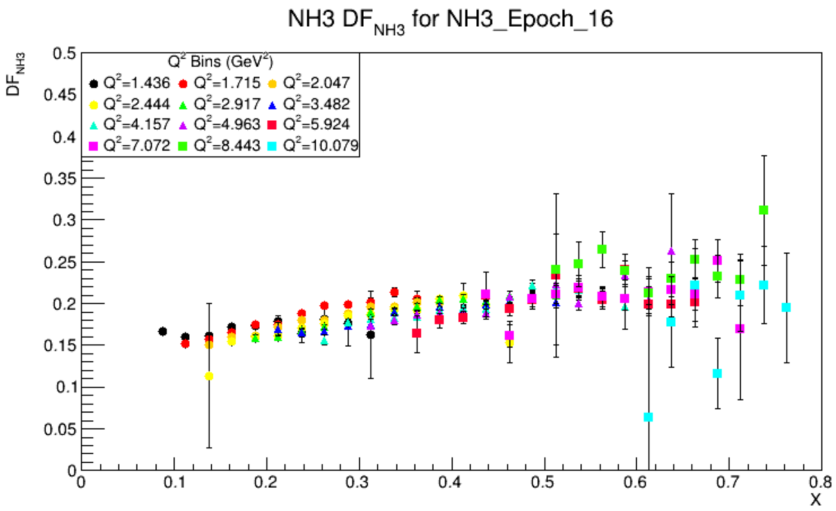

Spring 2023 D_F

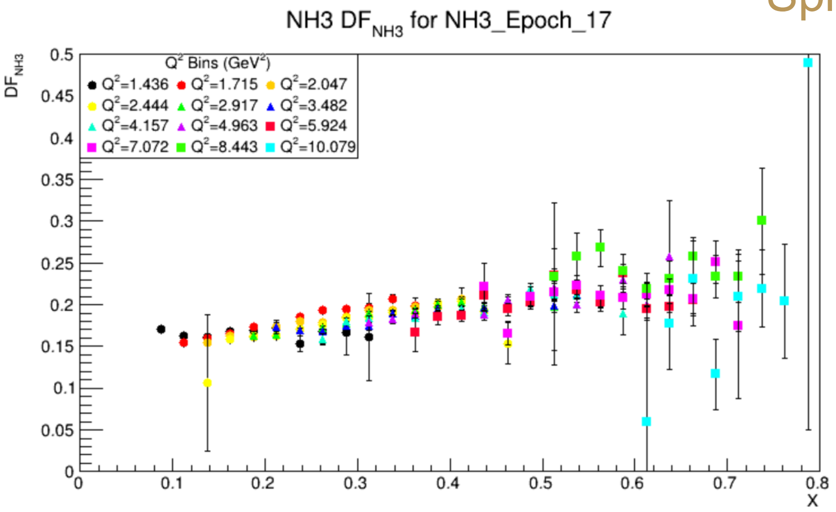

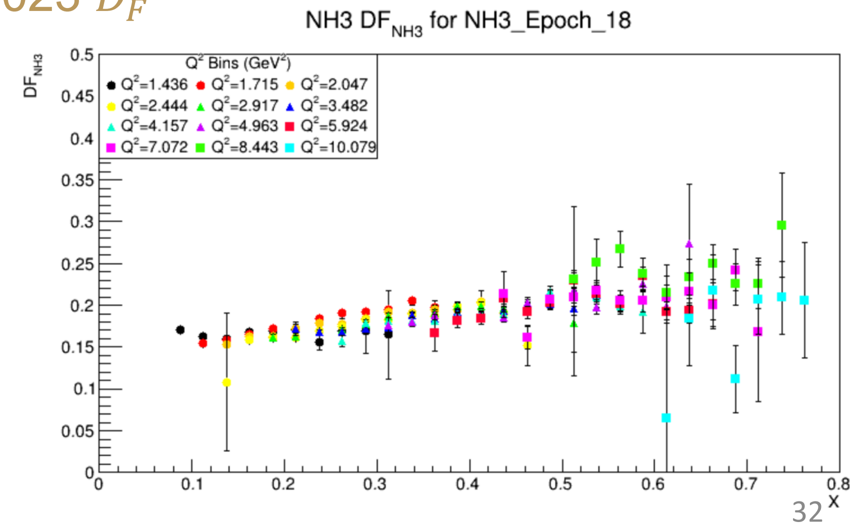

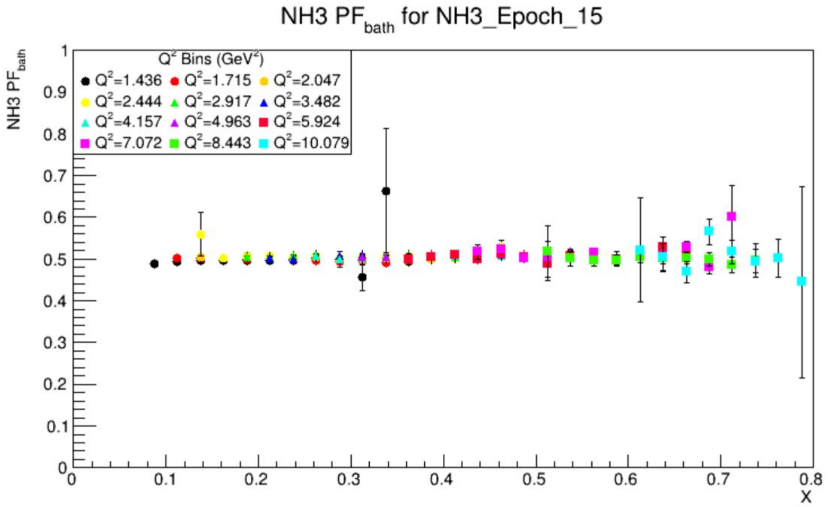

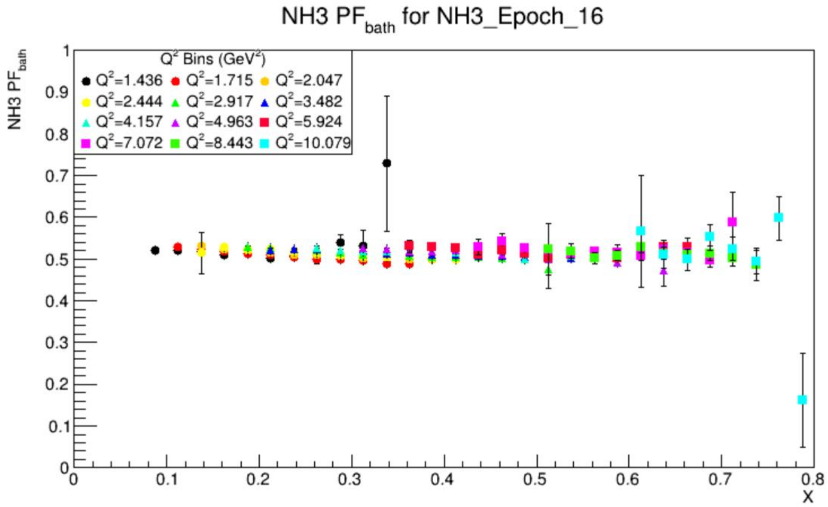

Spring 2023 P_F

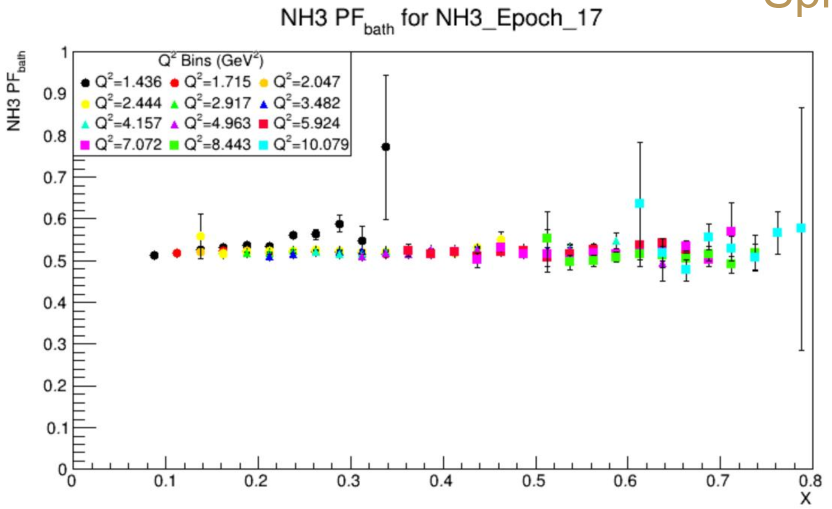

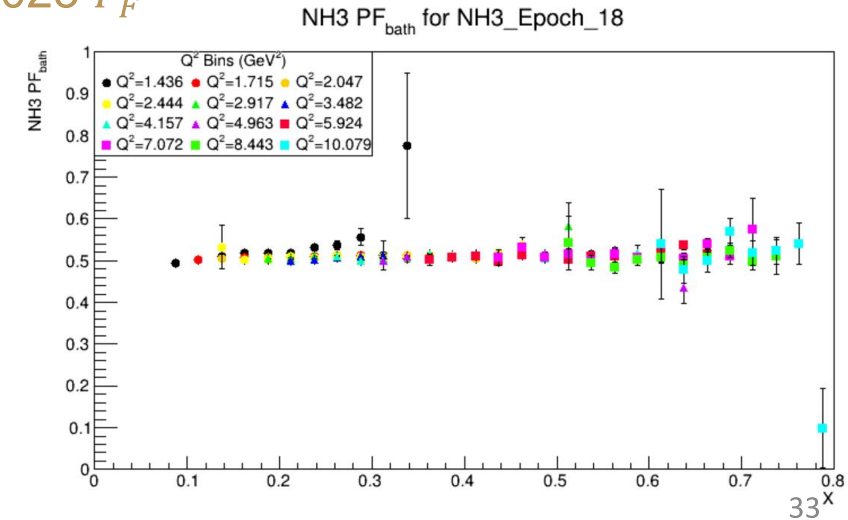

Issues with ND3 D_F

- $D_{F,ND3}$ deviated significantly from models as well as showed inconsistent behavior in the fall and spring data sets
- "Stratification" in the fall and spring data

- No CD2 runs were taken for summer and fall, so we had to generate pseudo-CD2 counts for the summer and fall datasets
- Scaled CH2 counts in the summer and fall using the CD2 and CH2 counts from the spring 23 dataset
- For each bin in x, Q^2 for summer/fall CH2 targets, multiplied counts by $\left(\frac{n_{CD2}}{n_{CH2}}\right)_{Sp23}$ to generate pseudo CD2:
- $(n_{CH2})_{SuFa22} * \left(\frac{n_{CD2}}{n_{CH2}}\right)_{Sp23} \approx (n_{CD2})_{SuFa22}$

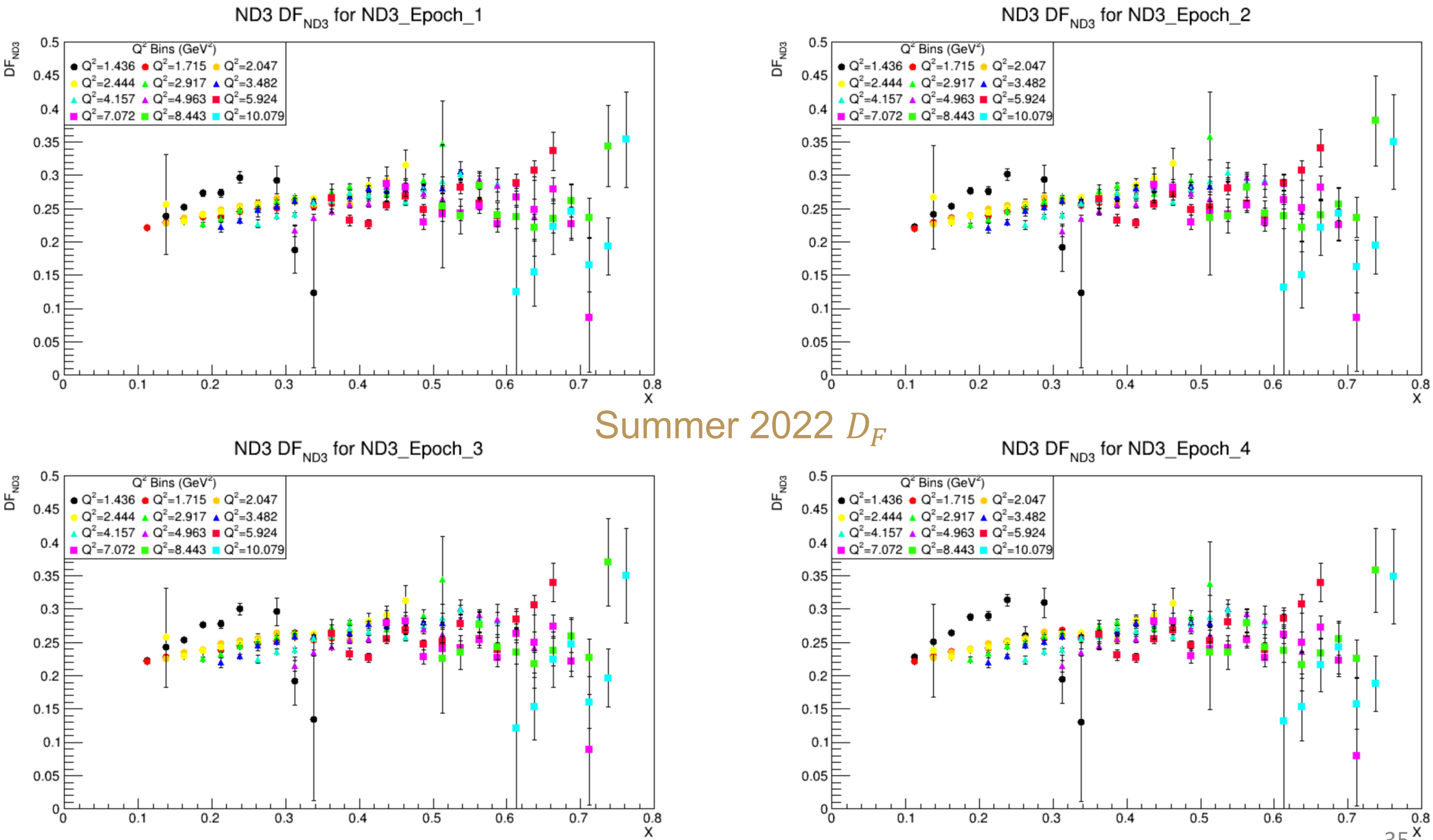

Summer 2022 D_F

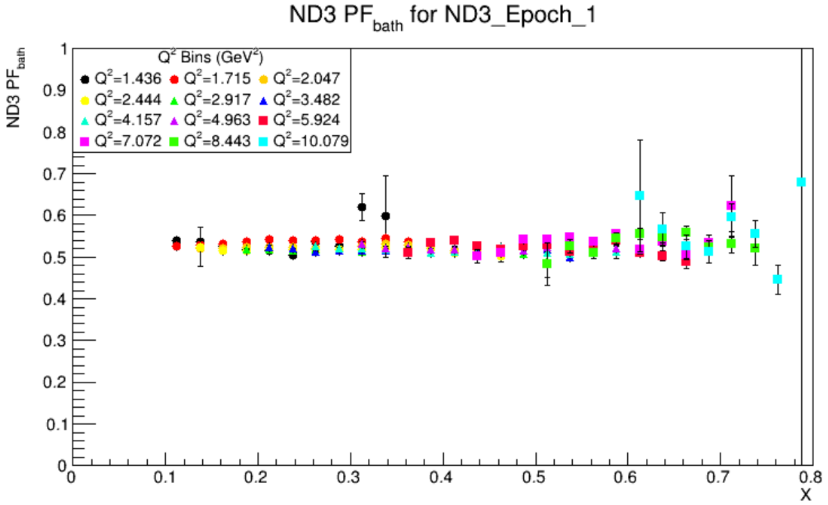

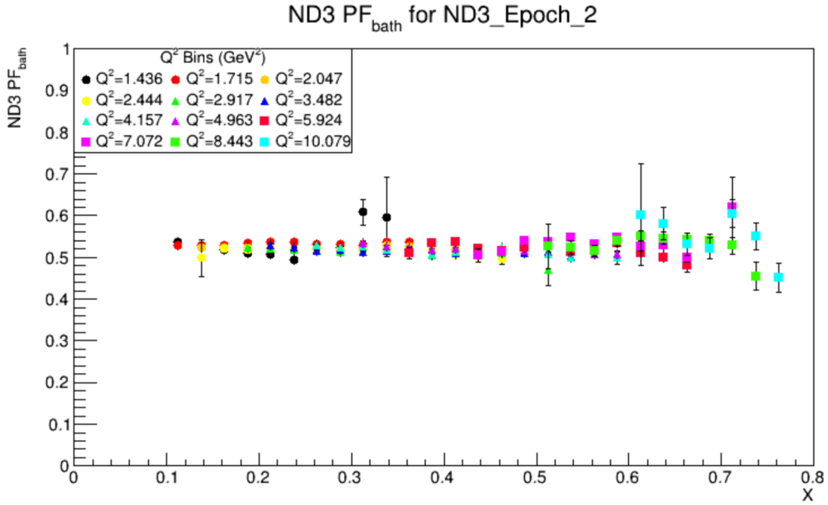

Summer 2022 P_F

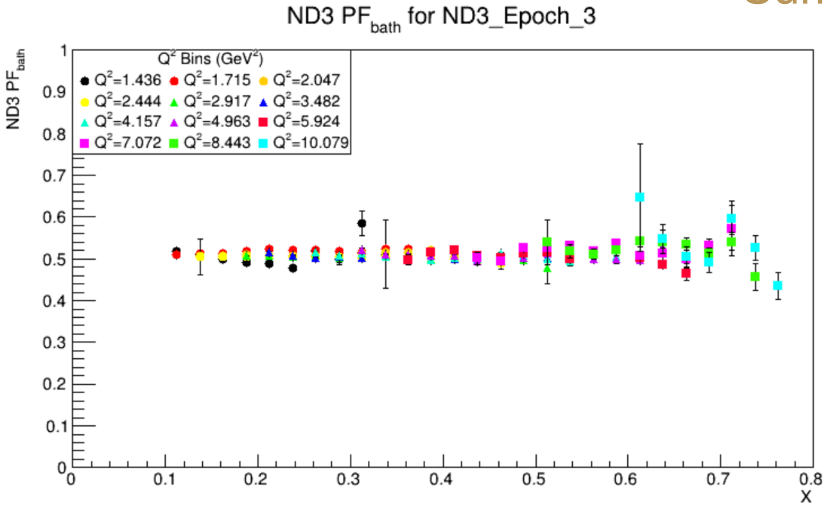

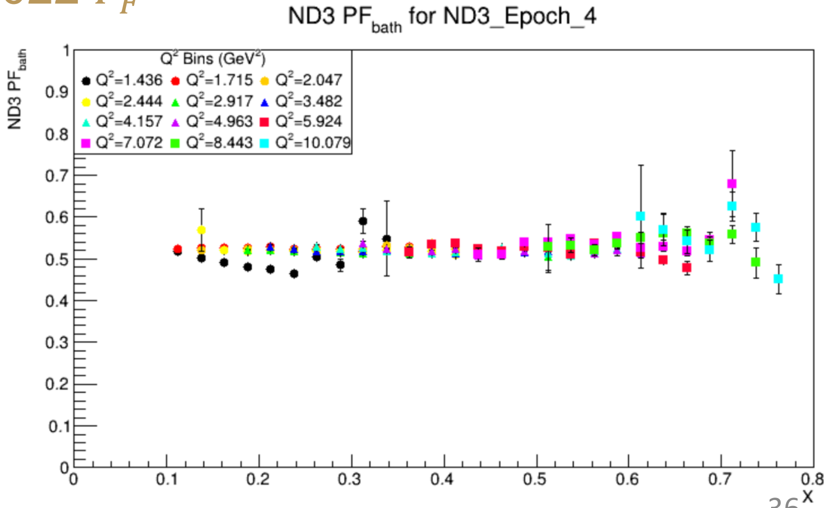

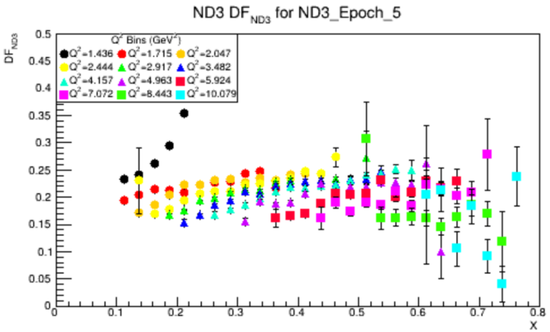
ND3 DF_ND3 for ND3_Epoch_5
DF_ND3
x
Q² Bins (GeV²)
Q²=1.436 Q²=1.715 Q²=2.047
Q²=2.444 Q²=2.917 Q²=3.482
Q²=4.157 Q²=4.963 Q²=5.924
Q²=7.072 Q²=8.443 Q²=10.079

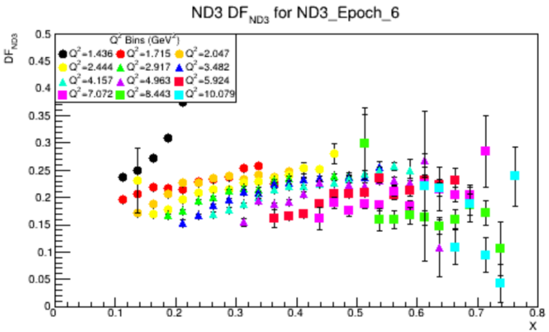
ND3 DF_ND3 for ND3_Epoch_6
DF_ND3
x
Q² Bins (GeV²)
Q²=1.436 Q²=1.715 Q²=2.047
Q²=2.444 Q²=2.917 Q²=3.482
Q²=4.157 Q²=4.963 Q²=5.924
Q²=7.072 Q²=8.443 Q²=10.079

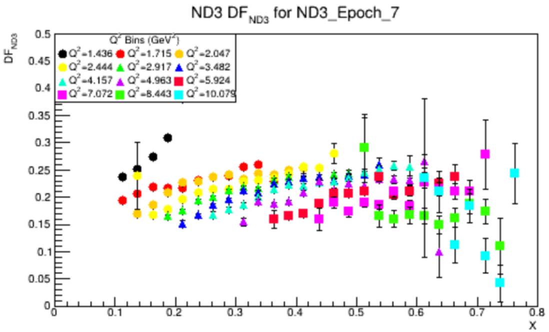
ND3 DF_ND3 for ND3_Epoch_7
DF_ND3
x
Q² Bins (GeV²)
Q²=1.436 Q²=1.715 Q²=2.047
Q²=2.444 Q²=2.917 Q²=3.482
Q²=4.157 Q²=4.963 Q²=5.924
Q²=7.072 Q²=8.443 Q²=10.079

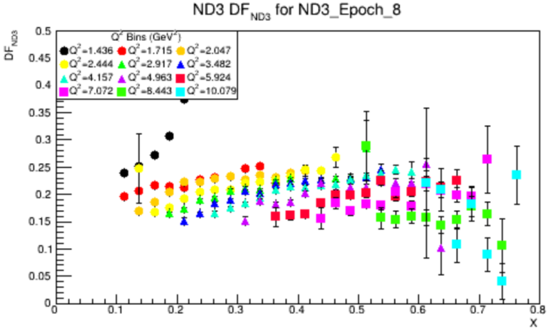
ND3 DF_ND3 for ND3_Epoch_8
DF_ND3
x
Q² Bins (GeV²)
Q²=1.436 Q²=1.715 Q²=2.047
Q²=2.444 Q²=2.917 Q²=3.482
Q²=4.157 Q²=4.963 Q²=5.924
Q²=7.072 Q²=8.443 Q²=10.079

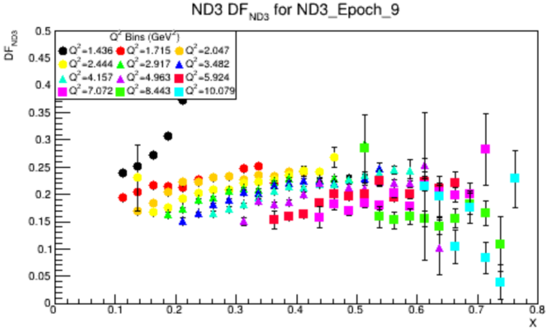
ND3 DF_ND3 for ND3_Epoch_9
DF_ND3
x
Q² Bins (GeV²)
Q²=1.436 Q²=1.715 Q²=2.047
Q²=2.444 Q²=2.917 Q²=3.482
Q²=4.157 Q²=4.963 Q²=5.924
Q²=7.072 Q²=8.443 Q²=10.079

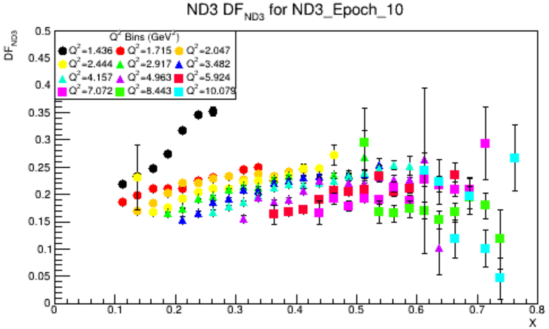
ND3 DF_ND3 for ND3_Epoch_10
DF_ND3
x
Q² Bins (GeV²)
Q²=1.436 Q²=1.715 Q²=2.047
Q²=2.444 Q²=2.917 Q²=3.482
Q²=4.157 Q²=4.963 Q²=5.924
Q²=7.072 Q²=8.443 Q²=10.079

Fall 2022 D_F

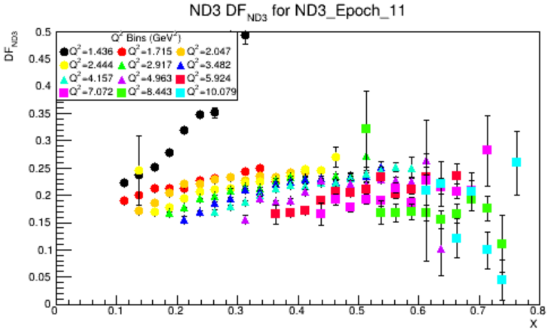
ND3 DF_ND3 for ND3_Epoch_11
DF_ND3
x
Q² Bins (GeV²)
Q²=1.436 Q²=1.715 Q²=2.047
Q²=2.444 Q²=2.917 Q²=3.482
Q²=4.157 Q²=4.963 Q²=5.924
Q²=7.072 Q²=8.443 Q²=10.079

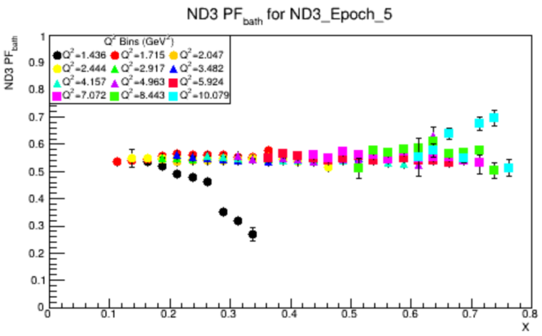
ND3 PF$_{bath}$ for ND3_Epoch_5
ND3 PF$_{bath}$
x
Q^2 Bins (GeV^2)
Q^2=1.436 Q^2=1.715 Q^2=2.047
Q^2=2.444 Q^2=2.917 Q^2=3.482
Q^2=4.157 Q^2=4.963 Q^2=5.924
Q^2=7.072 Q^2=8.443 Q^2=10.079

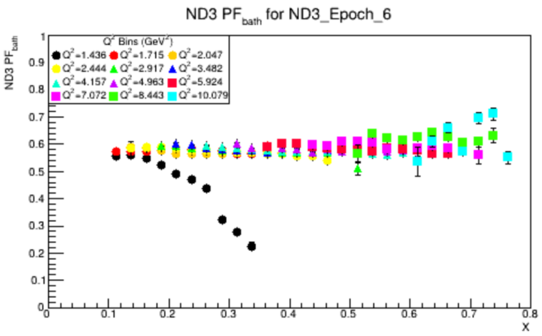
ND3 PF$_{bath}$ for ND3_Epoch_6
ND3 PF$_{bath}$
x
Q^2 Bins (GeV^2)
Q^2=1.436 Q^2=1.715 Q^2=2.047
Q^2=2.444 Q^2=2.917 Q^2=3.482
Q^2=4.157 Q^2=4.963 Q^2=5.924
Q^2=7.072 Q^2=8.443 Q^2=10.079

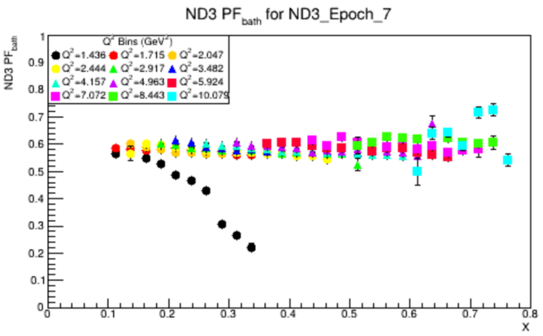
ND3 PF$_{bath}$ for ND3_Epoch_7
ND3 PF$_{bath}$
x
Q^2 Bins (GeV^2)
Q^2=1.436 Q^2=1.715 Q^2=2.047
Q^2=2.444 Q^2=2.917 Q^2=3.482
Q^2=4.157 Q^2=4.963 Q^2=5.924
Q^2=7.072 Q^2=8.443 Q^2=10.079

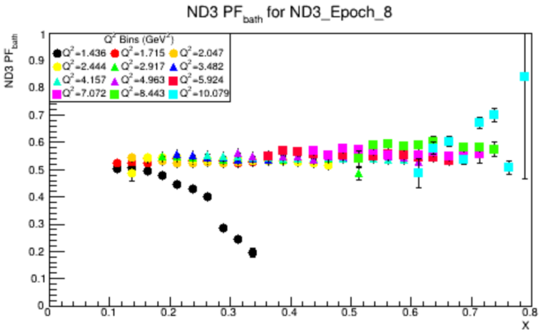
ND3 PF$_{bath}$ for ND3_Epoch_8
ND3 PF$_{bath}$
x
Q^2 Bins (GeV^2)
Q^2=1.436 Q^2=1.715 Q^2=2.047
Q^2=2.444 Q^2=2.917 Q^2=3.482
Q^2=4.157 Q^2=4.963 Q^2=5.924
Q^2=7.072 Q^2=8.443 Q^2=10.079

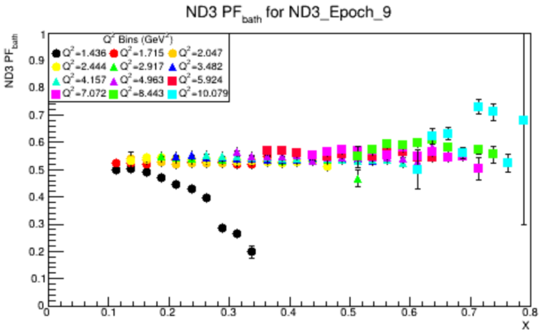
ND3 PF$_{bath}$ for ND3_Epoch_9
ND3 PF$_{bath}$
x
Q^2 Bins (GeV^2)
Q^2=1.436 Q^2=1.715 Q^2=2.047
Q^2=2.444 Q^2=2.917 Q^2=3.482
Q^2=4.157 Q^2=4.963 Q^2=5.924
Q^2=7.072 Q^2=8.443 Q^2=10.079

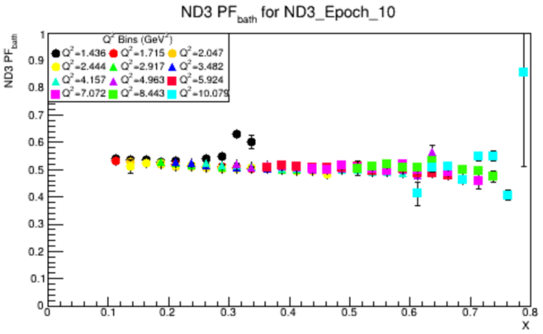
ND3 PF$_{bath}$ for ND3_Epoch_10
ND3 PF$_{bath}$
x
Q^2 Bins (GeV^2)
Q^2=1.436 Q^2=1.715 Q^2=2.047
Q^2=2.444 Q^2=2.917 Q^2=3.482
Q^2=4.157 Q^2=4.963 Q^2=5.924
Q^2=7.072 Q^2=8.443 Q^2=10.079

Fall 2022 P_F

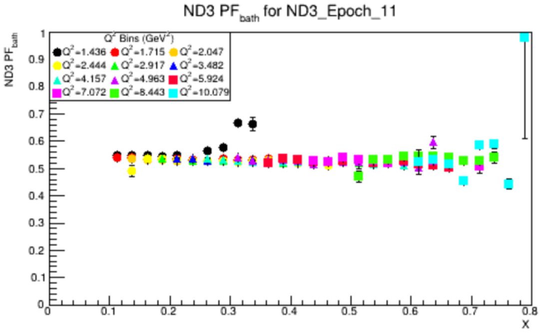
ND3 PF$_{bath}$ for ND3_Epoch_11
ND3 PF$_{bath}$
x
Q^2 Bins (GeV^2)
Q^2=1.436 Q^2=1.715 Q^2=2.047
Q^2=2.444 Q^2=2.917 Q^2=3.482
Q^2=4.157 Q^2=4.963 Q^2=5.924
Q^2=7.072 Q^2=8.443 Q^2=10.079

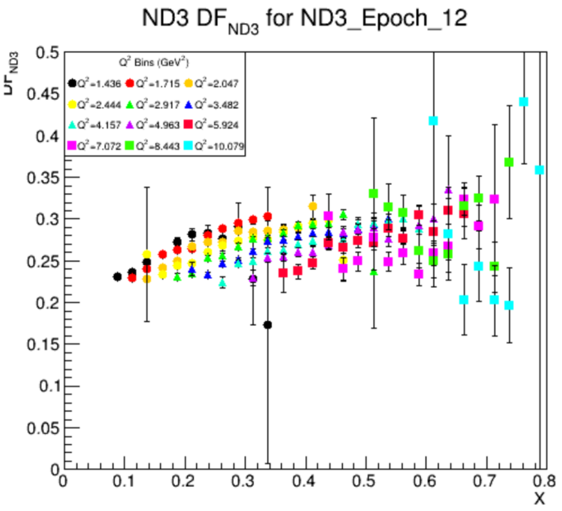

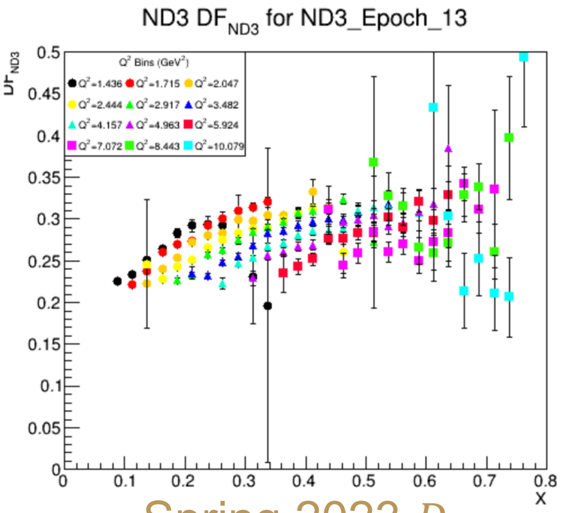

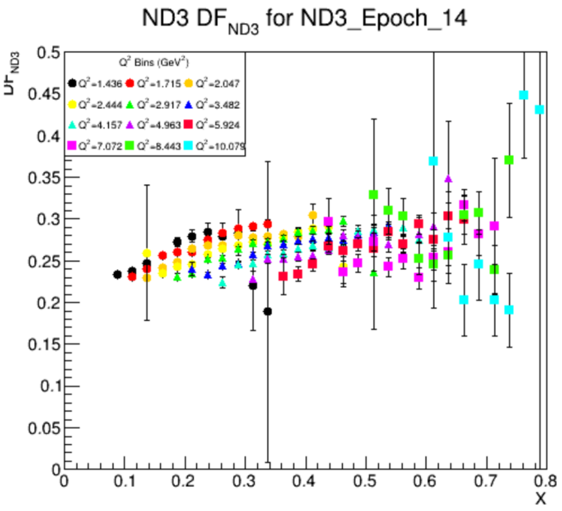

Spring 2023 D_F

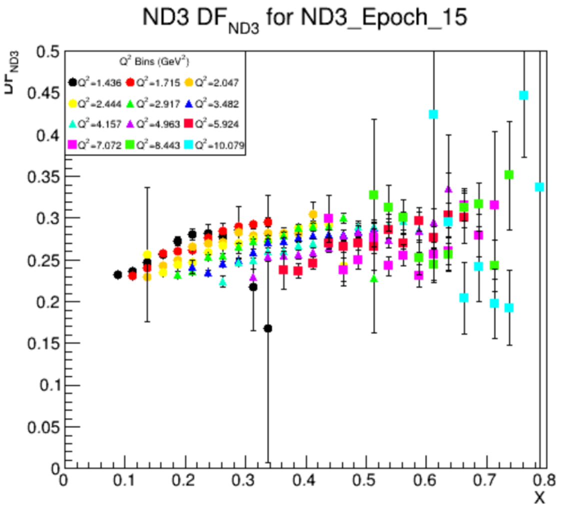

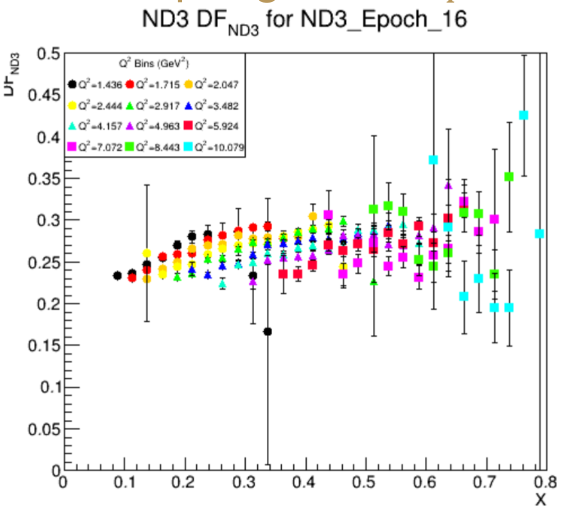

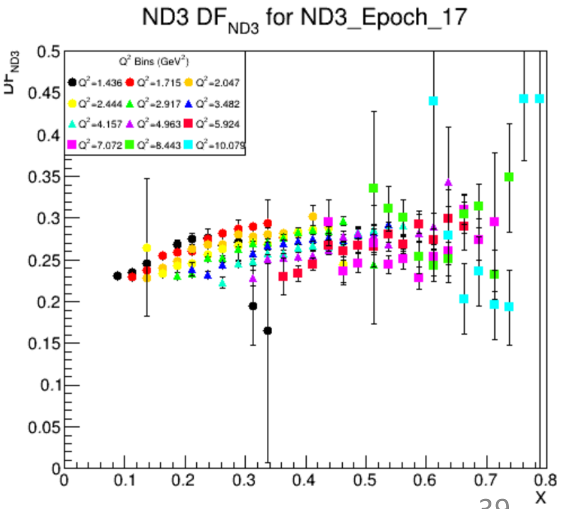

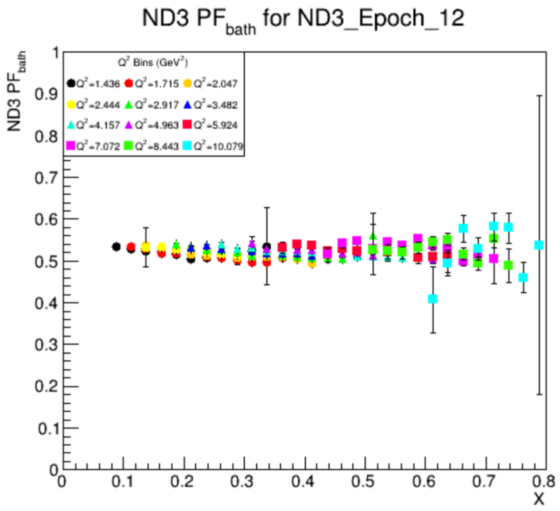

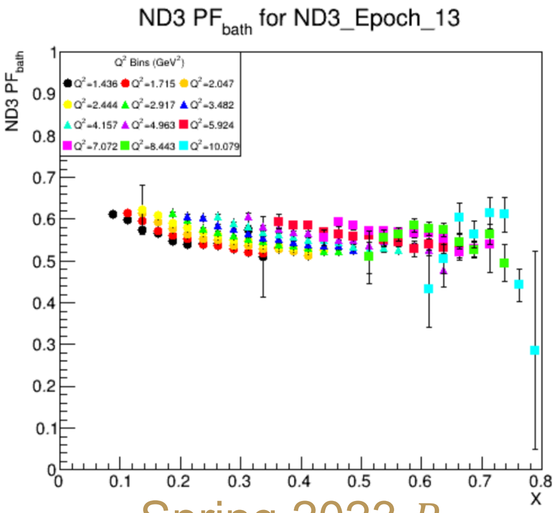

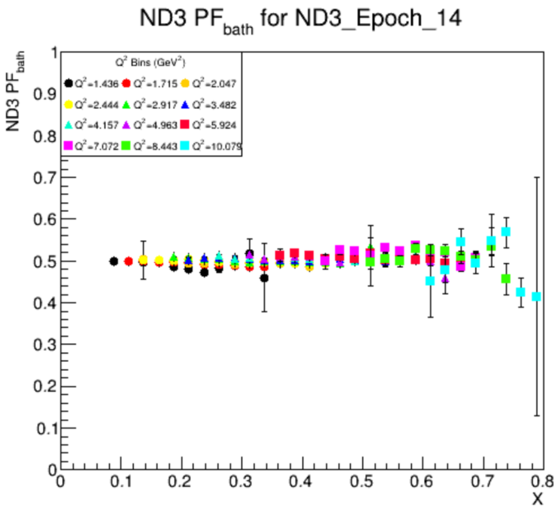

Spring 2023 P_F

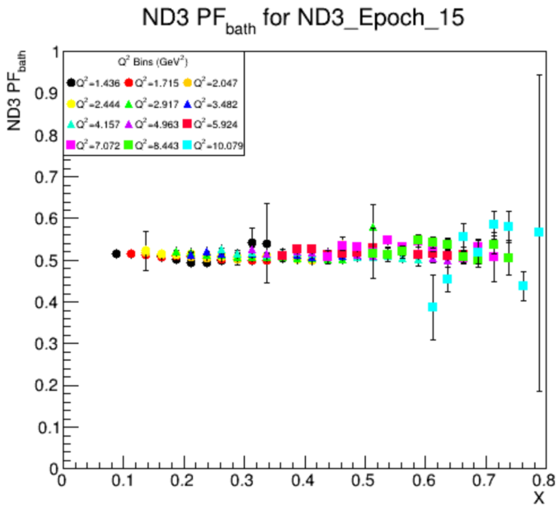

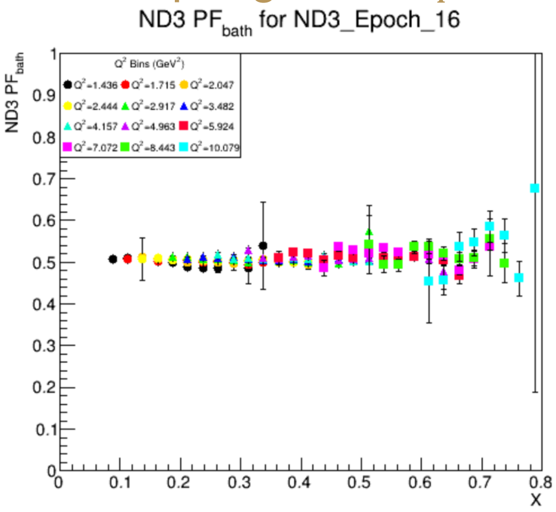

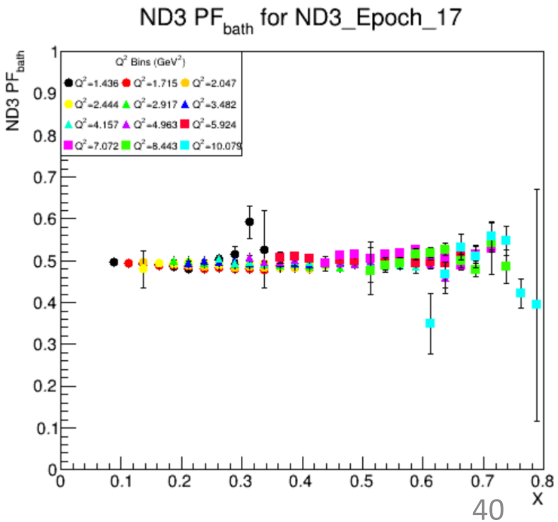

Virtual Photon Asymmetries

$$A_1 \equiv \frac{(\sigma_{1/2} - \sigma_{3/2})}{(\sigma_{1/2} + \sigma_{3/2})} \qquad A_2 \equiv \frac{2\sigma_{LT}}{(\sigma_{1/2} + \sigma_{3/2})}$$

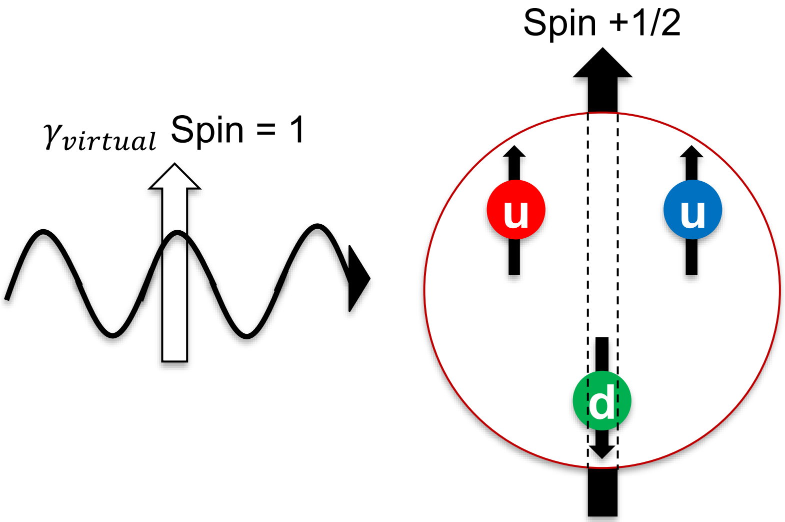

$\sigma_{3/2}$ Cross Section

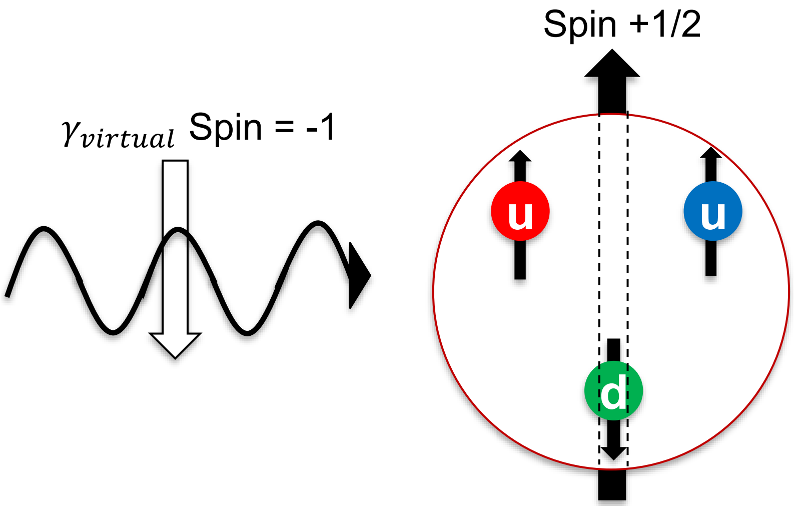

$\sigma_{1/2}$ Cross Section

Virtual Photon Asymmetries

- $\sigma_{LT} \propto \gamma[g_1 + g_2]$, $\quad (\sigma_{1/2} - \sigma_{3/2}) \propto (g_1 - \gamma^2 g_2)$, $\quad (\sigma_{1/2} + \sigma_{3/2}) \propto F_1$

$$\boldsymbol{A_1 \equiv \frac{(\sigma_{1/2} - \sigma_{3/2})}{(\sigma_{1/2} + \sigma_{3/2})} \quad A_2 \equiv \frac{2\sigma_{LT}}{(\sigma_{1/2} + \sigma_{3/2})}}$$

Virtual Photon Asymmetries

- $\sigma_{LT} \propto \gamma[g_1 + g_2], \quad (\sigma_{1/2} - \sigma_{3/2}) \propto (g_1 - \gamma^2 g_2), \quad (\sigma_{1/2} + \sigma_{3/2}) \propto F_1$

$$A_1 = \frac{g_1 - \gamma^2 g_2}{F_1} \qquad A_2 = \frac{\gamma[g_1 + g_2]}{F_1}$$

- $\gamma = 2M_p x/Q^2$ As $Q^2 \to \infty, \quad A_1 \approx g_1/F_1$
- F_1 **unpolarized structure function** (scattering probability)
- g_1 **spin structure function** (scattering probability asymmetry based on spin)

g_1 describes the proton's longitudinal spin structure!

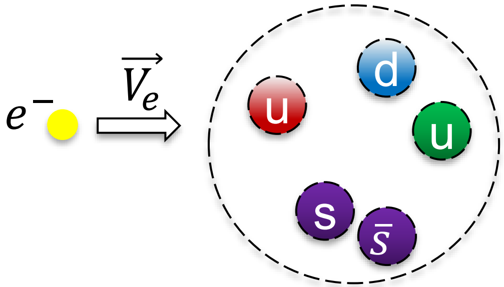

Probability:
$P_u(x) = ?$
$P_d(x) = ?$
$P_s(x) = ?$
$P_{\bar{s}}(x) = ?$
$\propto F_1$

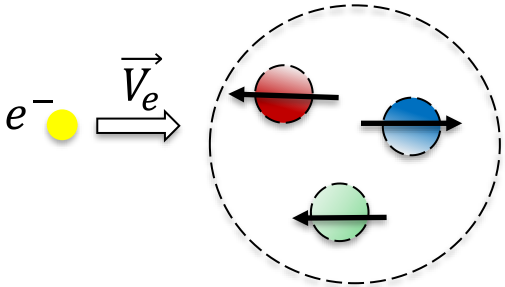

Probability:
$P_{q\uparrow}(x) - P_{q\downarrow}(x) \propto g_1$

Dynamic Nuclear Polarization

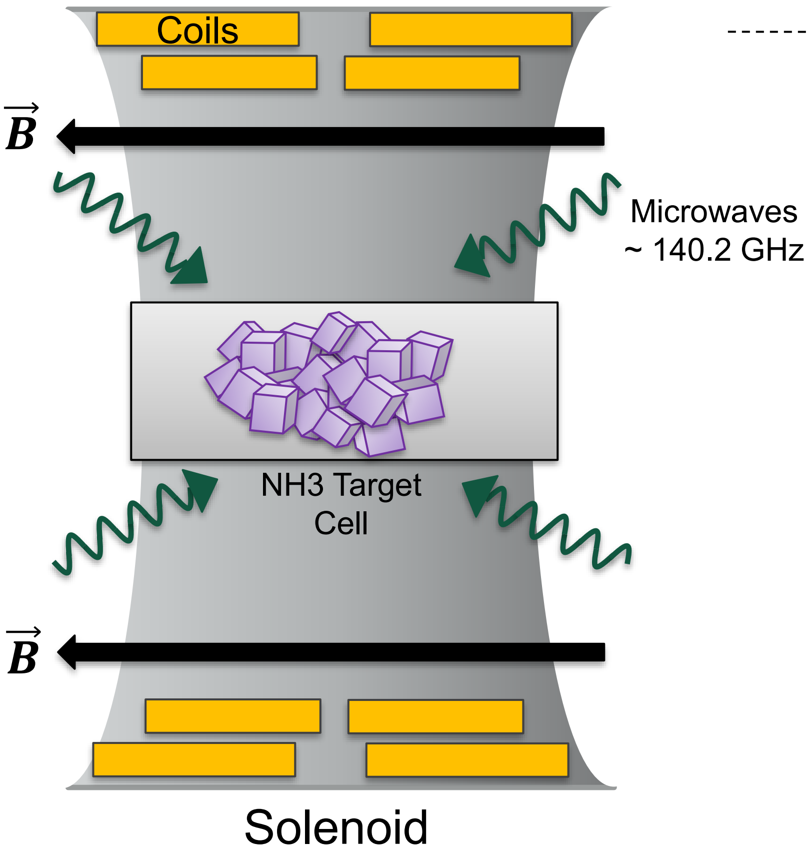

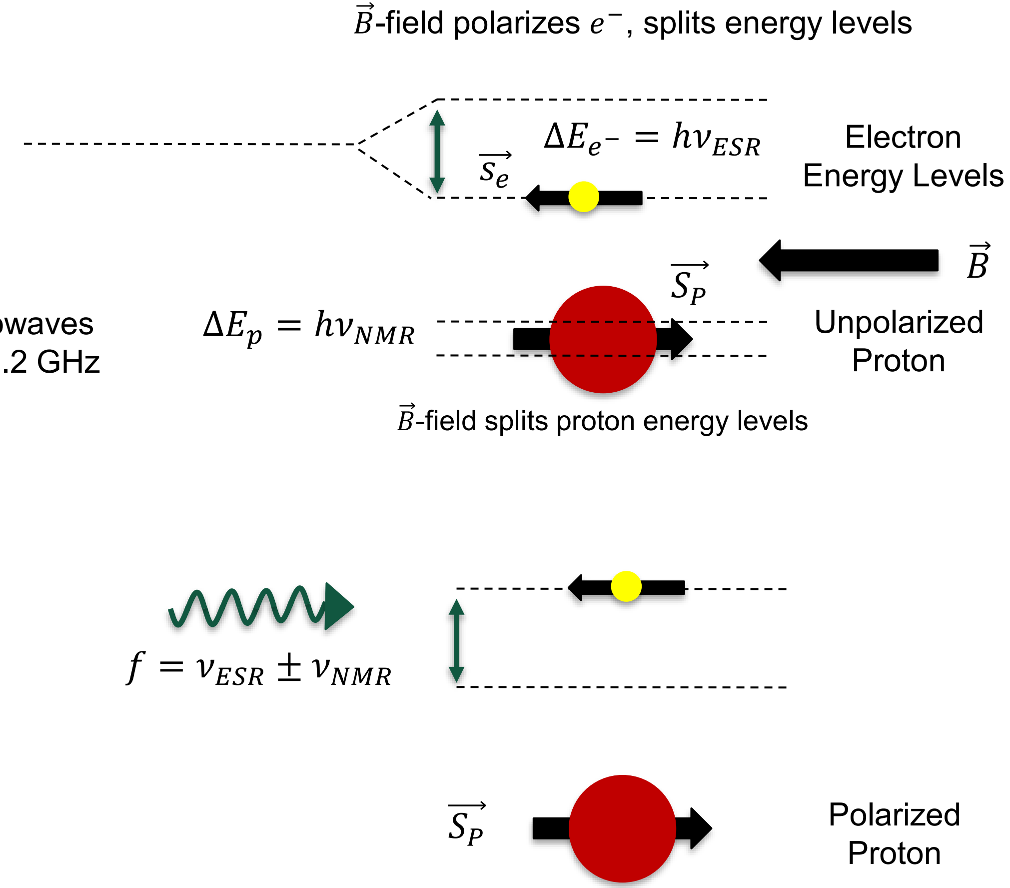

Beam-Target Polarization Calculations

$$A_{||,phys} = \frac{A_{||,raw}}{D_F P_b P_t} \quad \Rightarrow \quad P_b P_t = \frac{A_{||,raw}}{D_F A_{||,phys}}$$

- Use a model to calculate $A_{||,phys}$
- Values of $P_b P_t$ were calculated for RGC data using exclusive elastic $ep \rightarrow e'p'$ scattering (Noemie Pilleux)

$$P_b P_t = \frac{\sum_{Q^2\ bins} d_{f,i} A_{th,i}(n_i^- - n_i^+)}{\sum_{Q^2\ bins} d_{f,i}^2 A_{th,i}^2 (n_i^- + n_i^+)}$$

- d_f = separate dilution factor, A_{th} = elastic asymmetry parameterized by Arrington et. al.

$$A_{th} = \frac{2\tau r_g [M/E + r_G(\tau M/E + (1+\tau)\tan^2(\theta/2))]}{1 + r_G^2 \tau/\epsilon} \qquad r_g \equiv G_M/G_E$$

- For DIS $P_b P_t$, calculated in x, Q^2 bins using $A_{th} = D(A_1 + \eta A_2)$, with Values of D, η, A_1, A_2 come from S. Kuhn 's model
- Much greater statistics than elastic

$$P_b P_t = \frac{\sum_{x,Q^2\ bins} D_{f,i} A_{th,i}(n_i^- - n_i^+)}{\sum_{x,Q^2\ bins} D_{f,i}^2 A_{th,i}^2 (n_i^- + n_i^+)}$$

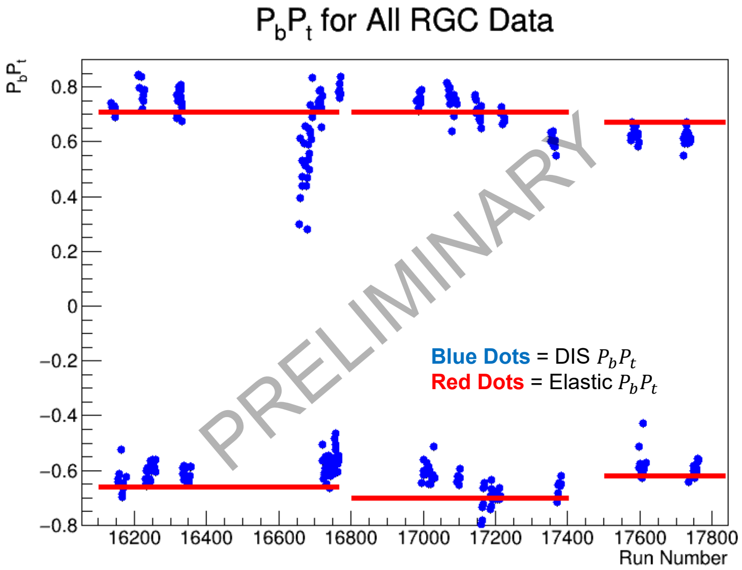

Normalize DIS $P_b P_t$ to elastic $P_b P_t$ to avoid circular calculation!